Stony Brook University

Caveolin-1 Localization and Trafficking and the Effect of Varying Bilayer Thickness on Caveolin-1 Hydrophobic Domain Topology in Model Membranes

A Thesis Presented

by

Catherine Peterson

to

The Graduate School

In Partial Fulfillment of the

Requirements

for the Degree of

Master of Arts

in

Biological Sciences

Stony Brook University

August 2009

Stony Brook University

The Graduate School

Catherine Maud Peterson

We, the thesis committee for the above candidate for the

Master of Arts degree, hereby recommend

acceptance of this thesis.

Dr. Deborah A. Brown - Thesis Advisor
Professor, Department of Biochemistry and Cell Biology

Dr. Erwin London
Professor, Department of Biochemistry and Cell Biology

Dr. Bernadette C. Holdener
Associate Professor, Department of Biochemistry and Cell Biology

This thesis is accepted by the Graduate School

Lawrence Martin
Dean of the Graduate School

Abstract of the Thesis

Caveolin-1 Localization and Trafficking and the Effect of Varying Bilayer Thickness on Caveolin-1 Hydrophobic Domain Topology in Model Membranes

by

Catherine Maud Peterson

Master of Arts

in

Biological Sciences

Stony Brook University

2009

Caveolae are normally seen as flask-shaped indentations present on the plasma membrane of most cell types. Caveolin-1 is a major protein associated with the formation and maintenance of caveolae and is also a key player in caveolar endocytosis. However, little is known about caveolin-1 trafficking and recycling. Here, in the first part of this thesis, we noted an unusual perinuclear localization pattern for over-expressed caveolin-1 and further investigated the observed perinuclear compartment using CTxB (cholera toxin subunit B) as a marker for caveolar endocytosis. This perinuclear compartment did not appear to colocalize with known Golgi markers, although it was located very close to the labeled Golgi structures. However, BFA (brefeldin A) treatment caused tubule formation by both the perinuclear compartment and the TGN (*trans*-Golgi network), so this compartment may be an unlabeled TGN subcompartment. In addition, transfection of the dominant negative myosin Vb tail, which prevents myosin Vb-dependent recycling, partially altered the localization pattern of caveolin-1 to a slightly

different amorphous perinuclear localization. However, the reason for this effect is currently unknown.

In previous studies, caveolae have been shown to flatten out in cholesterol-depleted membranes. Therefore, it is possible that caveolin-1 may change conformation in response to changes in lipid/sterol composition of the membrane bilayer, and thus may determine whether caveolae are flat or invaginated. Therefore, in the second part of this thesis, we synthesized a peptide corresponding to the caveolin-1 hydrophobic domain and used Trp fluorescence to study its topology in model membranes. After inserting the peptide into thin and thick membranes in the presence and absence of different quenchers, we obtained conflicting fluorescence results. The quenchers indicated that the fluorescing Trp was buried within the bilayer in thick membranes and located at the membrane border in thin bilayers. In contrast, although Trp fluorescence values in membranes without quenchers also indicated that in thin bilayers the Trp appeared to be at the bilayer border, while in thick bilayers the Trp fluorescence appeared to indicate that the Trp was exposed to a very aqueous environment. We propose a tentative model for how caveolin-1 induces membrane curvature in thick bilayers but not thin ones, but this model does not fully explain the contrasting results obtained in the two assays. We suggest that the hydrophobic domain may be able to form a hairpin loop in thinner membranes, whereas the it would be too short to form a hairpin in thicker membranes.

Table of Contents

List of Figures

List of Tables

Acknowledgements

First and foremost, I would like to thank Dr. Debbie Brown, my advisor, for her encouragement and patience throughout my work on this thesis. From the day I began work in her lab, Dr. Brown always had advice and was unerringly patient as I learned the necessary skills and background information needed to perform this research.

Thank you to Dr. Bernadette Holdener and Dr. Erwin London for being members of my committee. Special thanks to Dr. London for helping me sort through the caveolin-1 peptide data and figuring out what was happening in each experiment.

I would like to thank my fellow lab members, Anne Ostermeyer-Faye, Prakhar Verma and Azad Gucwa for their help and advice throughout my thesis work.

I also thank the W. M. Keck Small Scale Peptide Synthesis Center at Yale University for synthesizing the peptide used in these experiments.

Finally, I would like to thank my friends and family for their unconditional love and support throughout my thesis work.

Chapter 1: Caveolin-1 Localization and Trafficking

Introduction:

Caveolae are generally flask-shaped indentations present on the plasma membrane of most cell types, although the physiological status of the cells can affect caveolae morphology (Conner and Schmid, 2003; Thomas and Smart, 2008). In previous studies, caveolae have been shown to flatten out in cholesterol-depleted membranes (Rothberg et al., 1992; Tagawa et al., 2005). Caveolin-1 is a major protein associated with the formation and maintenance of caveolae. We believe that caveolin-1 may change conformation in response to changing lipid/sterol composition, and may determine whether caveolae are flat or invaginated. Caveolin-1 has a complex but poorly understood trafficking pathway in cells. We know that caveolin-1 is endocytosed and delivered to caveosomes, but it must also be recycled back to the plasma membrane and very little is known about this process and how it occurs. The long-term goal of these studies is to investigate caveolin-1 trafficking and discover what happens to it after delivery to the caveosomes.

In the process of transformation, the SKBr3 breast cancer cell line has lost the expression of caveolin-1 (Xie et al., 2003). When we re-expressed the protein in these cells by transient transfection, we found that the caveolin-1 localization pattern was slightly different than in normal cells. In SKBr3 cells caveolin-1 formed plasma membrane puncta (caveolae) and cytoplasmic caveosomes, a localization pattern that was virtually identical with that seen in normal cells. However, we saw more caveolin-1 in early endosomes than in normal cells. Caveolin-1 normally passes through early

endosomes during its transport cycle, but very little of the protein is present there at steady state (Pelkmans et al., 2004). In addition, re-expressed caveolin-1 (through transient transfection) often accumulated in an unusual amorphous perinuclear compartment in SKBr3 cells. Therefore, we hypothesized that SKBr3 cells might transport caveolin-1 normally, but that the rates of transport between specific compartments might be altered, which would result in a different pattern of steady-state localization.

Unfortunately, caveolin-1 lacks an extracellular domain, and so we could not directly determine the trafficking behavior of caveolin-1. Therefore we had to use an endocytic marker to indirectly study this behavior. Since SKBr3 cells still successfully internalize and traffic cholera toxin subunit B (CTxB) using the clathrin-dependent pathway, as well as non-clathrin, non-caveolar pathways, we wanted to use CTxB as an endocytic marker in SKBr3 cells, in order to determine whether various compartments labeled with transfected caveolin-1 could receive endocytosed cargo. In the course of these studies, we noticed that CTxB also labeled the novel perinuclear compartment.

Since SKBr3 cells exhibit a localization pattern that is mostly similar to, but has a few noticeable differences from, the localization pattern seen in normal cells, we hypothesized that the trafficking pathway of caveolin-1 is similar or the same in normal cells and SKBr3 cells, but that the rate of transport at various steps is different. Therefore, in SKBr3 cells, caveolin-1 accumulates abnormally in compartments that, in normal cells, it would normally pass through so rapidly that you don't see the protein there. If so, then defining what the functions of these compartments are could give valuable information on the normal cycling pathway of cav1. Since the perinuclear

compartment has not been observed in normal cells, I characterized this compartment in more detail. As part of this effort I used transient transfections to over-express caveolin-1, as well as several other markers, and internalized cholera toxin and transferrin under a variety of different conditions to determine which endocytic compartments were associated with caveolar endocytosis. In addition, I used several different drugs (brefeldin A, methyl-β-cyclodextrin, and cycloheximide) in an attempt to determine whether this perinuclear compartment was endocytic or biosynthetic. I also transfected a dominant-negative form of myosin Vb to try and establish whether or not this was a recycling compartment.

Mechanisms of Endocytosis

Cells use several different methods of endocytosis, which fall into two major categories: phagocytosis and pinocytosis (Conner and Schmid, 2003; Ridley, 2001). While phagocytosis is limited to certain specialized cells in mammals, all cells undergo pinocytosis through at least four different pathways: macropinocytosis, clathrin-mediated endocytosis, caveolae-mediated endocytosis and clathrin- and caveolae-independent endocytosis (Conner and Schmid, 2003). These pathways function to tightly regulate complex physiological processes including hormone-mediated signal transduction and antigen presentation, as well as govern the entry and exit of specific macromolecules, through a diverse set of mechanisms (Conner and Schmid, 2003). We would like to further characterize the trafficking behavior of a key endocytic protein, caveolin-1, to determine how it is trafficked through the cell. In the course of these studies, we identified an unusual perinuclear localization pattern for caveolin-1 and attempted to characterize this perinuclear compartment. As part of this endeavor, we tried to

determine which endocytic cargoes, if any, from the different pathways detailed below were transported to this compartment.

Macropinocytosis

Macropinocytosis occurs during the process of membrane ruffling induced by the stimulation of many different cell types through various signals, including growth factors (Conner and Schmid, 2003; Ridley, 2001). During macropinocytosis, the plasma membrane forms protrusions, which surround a region of extracellular fluid (Doherty and McMahon, 2009). These protrusions fall back onto and fuse with the plasma membrane, forming large vesicles known as macropinosomes that appear to contain the entire enclosed region of extracellular fluid (Conner and Schmid, 2003; Doherty and McMahon, 2009).

Clathrin-Mediated Endocytosis

Clathrin-mediated endocytosis regulates the constant uptake of essential nutrients and the endocytosis of many transmembrane receptors, such as the transferrin receptor, through the action of clathrin-coated pits (Brodsky et al., 2001; Conner and Schmid, 2003; Ridley, 2001). In addition, clathrin-coated vesicles are also known to aid in protein sorting in the *trans*-Golgi network during the creation of secretory vesicles and lysosomes (Brodsky et al., 2001).

Once the endocytic vesicles have formed, they rapidly travel to and fuse with early endosomes, which either rapidly recycle the cargo, or fuse together to form larger sorting endosomes (Sorkin and Goh, 2008). As the endosomes mature from early endosomes to multivesicular bodies and late endosomes, they undergo changes in both biochemical composition and morphology, which allows for the simultaneous sorting of

the internalized receptors and ligands to different destinations within the cell, including the Golgi, lysosomes and the endoplasmic reticulum (ER) (Alberts et al., 2007; Sorkin and Goh, 2008).

Caveolae-Mediated Endocytosis

Different cell types have greatly differing numbers of caveolae. Caveolae in adipocyte membranes, for example, may increase the total plasma membrane surface area by up to 50% (Thorn et al., 2003) whereas caveolae in fibroblast plasma membranes may increase the total surface area by only 3-5% (Guillot et al., 1990). Caveolae-mediated endocytosis occurs through recognition of the cargo molecules by caveolae (Conner and Schmid, 2003). Caveolae associate with cholesterol and sphingolipid-rich microdomains of the plasma membrane, where many signaling molecules and membrane transporters are also located (Conner and Schmid, 2003).

Although caveolae are normally stable at the plasma membrane, they can undergo endocytosis in response to specific triggers. Once internalized by this mechanism, caveolae form endocytic caveolar vesicles. These normally fuse with either the caveosome or the early endosome, but may occasionally be recycled back to the plasma membrane without fusing (Parton and Simons, 2007; Pelkmans and Zerial, 2005). However, very little is known about caveolin-1 trafficking and how it is recycled back to the plasma membrane (Parton and Simons, 2007). An important goal of the first part of my thesis is to learn more about this process.

Clathrin- and Caveolae-Independent Endocytosis

Clathrin- and caveolae-independent endocytosis occurs in a cholesterol-dependent manner and results in the internalization of cholera toxin, the GM1 receptor and GPI-

linked proteins, as well as many other receptors and molecules through multiple pathways (Doherty and McMahon, 2009). The best characterized of these is the CLIC/GEEC pathway, which delivers the cargo to GEECs (GPI-associated protein enriched early endosomes) by way of highly prevalent structures (CLICS) which exhibit a tubular or ring-like morphology (Doherty and McMahon, 2009).

Cholera Toxin Trafficking

Cholera toxin is a member of the AB_5-subunit toxin family, which also includes Shiga toxin and Verotoxin. It is composed of an A-subunit, formed from a single chain cleaved into two peptides (A1 and A2), and pentameric ring-like B-subunit formed from five identical peptides (Lencer and Tsai, 2003; Parton and Richards, 2003). The A- and B-subunits are connected by the C-terminus of the A2 chain, which also contains a KDEL motif that targets the complex to the endoplasmic reticulum (ER) (Lencer and Tsai, 2003). The B-subunit binds up to five identical plasma membrane gangliosides, specifically the oligosaccharide domain of the lipid-raft associated glycolipid receptor GM1, and triggers endocytosis, while the A1 chain eventually enters the cytosol from the ER and causes disease (Lencer and Tsai, 2003; Parton and Richards, 2003).

In order to enter the cell, the B-subunit first binds plasma membrane GM1 (whether it is bound to the A-subunit or not), and triggers endocytosis by both clathrin-dependent and clathrin-independent pathways, including caveolar endocytosis (Sandvig and van Deurs, 2002). The complex then proceeds to the early endosomes (and may continue to the late endosomes), before moving into the Golgi and being transported to the ER in a process known as retrograde transport (Majoul et al., 1998; Majoul et al., 1996; Parton and Richards, 2003). Retrograde transport between endosomes and the

Golgi occurs as a natural part of receptor trafficking, and is driven by a protein complex that includes clathrin, the Golgi clathrin adaptor AP-1, and epsinR, which cycles constitutively between endosomes and the *trans*-Golgi network (Johannes and Popoff, 2008). Since transport from the Golgi to the ER occurs in the opposite direction from the cell's standard secretory pathway, the cholera toxin complex hijacks the retro-translocation pathway normally used to recover escaped ER proteins, through the KDEL sequence on the A2 chain. Once the complex reaches the ER, the A-subunit separates from the B-subunit and is recognized as a misfolded protein by the resident chaperone proteins and is transported across the membrane to be degraded, at which point it evades the proteosome and ribosylates the Gs alpha subunit of the heterotrimeric G protein resulting in constitutive cAMP production (Hazes and Read, 1997; Tsai et al., 2002). This leads to increased ion secretion from intestinal epithelial cells, causing severe dehydration. In addition, another AB_5-subunit protein, shiga toxin, is transported from the early endosomes to the *trans*-Golgi network via what is believed to be a retromer-regulated pathway (Popoff et al., 2007), and it is possible that CTxB also takes advantage of this mechanism. Since the B-subunit follows the same pathway as the intact toxin without the associated toxicity, here we used the B-subunit alone (CTxB).

To summarize, having discovered an unusual perinuclear localization pattern for caveolin-1, in the first part of my thesis I have attempted to characterize this novel compartment. The important questions that I sought to answer are whether this compartment is an endocytic, a biosynthetic or a recycling compartment, and whether or not it is associated with the *trans*-Golgi network and/or Golgi.

Methods and Materials:

Immunofluorescence

SKBr3 cells were plated on coverslips at a density of $5x10^5$ cells/coverslip. The cells were transfected with 1 μg DNA of each plasmid 24 hours after plating and each experiment was performed ~40 hours after transfection. The cells were treated with relevant drugs and/or ligands, then fixed with 3% PFA (paraformaldehyde; 3% w/v paraformaldehyde in 1X PBS (phosphate-buffered saline), pH 8.0) for 30 minutes and permeabilized with 0.5% Triton X-100 for 5 minutes. The cells were blocked with 3% BSA (bovine serum albumin; 3% BSA in 1X PBS with 10 mM glycine) for either one hour at room temperature or overnight at 4°C, then incubated with the primary antibodies for one hour and the secondary antibodies for 30 minutes at room temperature. The coverslips were mounted on slides with 25 μL mounting media and sealed with clear nail polish. The cells were visualized with a 100x oil immersion objective.

Plasmids

The plasmids used were GFP-tagged caveolin-1, HA-tagged caveolin-1, RFP-tagged caveolin-1, GFP-tagged myosin Vb tail and YFP-tagged galactosyl transferase (a Golgi-targeted enzyme used as a Golgi marker).

Drugs and Ligands

Where indicated, the cells were treated with 10 μg/mL brefeldin A (BFA) for one hour at 37°C or with 10 mM methyl-β-cyclodextrin (MBCD) in DMEM for 20 or 45 minutes at 37°C. Protein synthesis was inhibited by treating the cells with 100 μg/mL cycloheximide for one hour at 37°C. Where indicated, the cells were also treated with Alexa Fluor 488- or Alexa Fluor 594-labeled CTxB (Invitrogen) and/or FITC-labeled red

or green transferrin for 5, 20 or 60 minutes at 37°C. CTxB and transferrin stock solutions were diluted in DMEM tissue culture media (containing 10% calf serum and 1% penicillin/streptomycin) to obtain the final concentrations of 10 µg/mL CTxB and 50 µg/mL transferrin. Ten mg/mL ruby red dextran was diluted 1:10 in DMEM to obtain the final concentration of 1 mg/mL and was internalized for 20 minutes at 37°C.

Antibodies

Both primary and secondary antibodies were diluted in PBS. Primary antibodies used were rabbit anti-HA (Santa Cruz) at 1:100, rabbit anti-Flag (Affinity Bio Reagents) at 1:200, sheep anti-TGN46 (AbD Serotec) at 1:50, rabbit anti-caveolin at 1:200, and mouse anti-EEA1 (BD Transduction Laboratories) at 1:100. Secondary antibodies used were Alexa Fluor 594 (goat anti-rabbit, goat anti-mouse and donkey anti-sheep) at 1:500 dilution, Alexa Fluor 488 (goat anti-rabbit and goat anti-mouse) at 1:800 dilution, and Alexa Fluor 350 (goat anti-rabbit) at 1:200 dilution. All secondary antibodies were obtained from Invitrogen.

Results:

Localization of CTxB in SKBr3 breast cancer cells

Although our goal was to investigate caveolin-1 trafficking in SKBr3 cells, since caveolin-1 does not have an extracellular domain we had to use a surrogate marker, cholera toxin subunit B (CTxB), to follow caveolar endocytosis. While CTxB is normally endocytosed through clathrin-dependent and clathrin-independent pathways, including the caveolar pathway (Lencer and Tsai, 2003), it is the only marker that has currently been shown to take advantage of caveolar endocytosis (Nichols, 2003). CTxB has been found localized at the plasma membrane, in early and late endosomes, and in the Golgi in a time-dependent manner (Majoul et al., 1998; Majoul et al., 1996; Richards et al., 2002). Since these studies were performed using various other cell lines, we began by confirming these results in order to verify that CTxB was endocytosed normally in SKBr3 cells. We chose to use SKBr3 cells because they lack endogenous caveolin-1, and therefore by transfecting them with caveolin-1, we could compare untransfected cells with transfected cells in order to determine whether the presence of caveolin-1 altered the localization patterns of different endocytosis markers. We internalized 10 μg/mL CTxB in SKBr3 breast cancer cells for 20 or 60 minutes (Fig. 1.1). As expected, we saw good colocalization between CTxB and EEA1-labeled endosomes after 20 minutes of internalization (Fig. 1.1A). However, when we looked at CTxB localization after 60 minutes of internalization using two different Golgi markers (TGN46, a *trans*-Golgi protein and GM130, a *cis*-Golgi matrix protein), we found unexpected results (Fig. 1.1B and C). Although we saw partial colocalization of CTxB with both Golgi markers, we

also saw that CTxB and the Golgi markers appeared to be partially localized to separate but adjacent compartments.

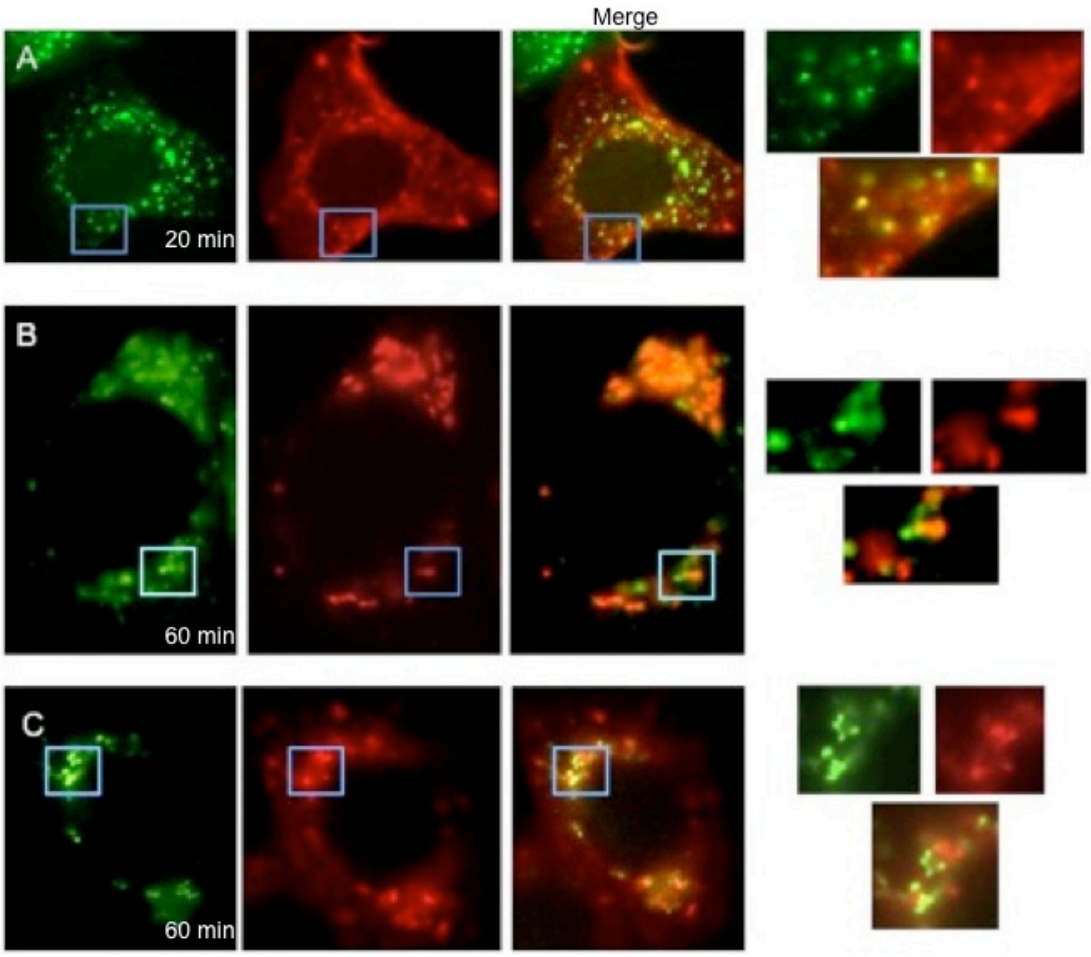

Figure 1.1. Confirmation of CTxB colocalization from previous studies. A: 20 minute CTxB internalization where CTxB is stained red and EEA1 is stained green, B: 60 minute CTxB internalization where CTxB is stained green, TGN46 (a *trans*-Golgi network protein) is stained red, and C: 60 minute CTxB internalization where CTxB is stained red and GM130 (a *cis*-Golgi network protein) is stained green.

Since transferrin is endocytosed via the clathrin-mediated pathway and caveolin-1 is associated with caveolar endocytosis, we wanted to verify whether CTxB was endocytosed by one or both of these pathways, and/or whether it had a different pathway in SKBr3 cells from those previously characterized. We speculated that CTxB internalization might be relatively non-specific, taking advantage of any available

endocytic pathway, and therefore we predicted that it would partially localize with transferrin. To investigate we internalized CTxB for 5, 20 and 60 minutes alone or with transferrin (which we used as a marker for clathrin-mediated endocytosis), and looked at colocalization of CTxB and transferrin (Fig. 1.2) and CTxB and caveolin-1 (Fig. 1.3). CTxB showed good colocalization with transferrin after 5 minutes of internalization, colocalized almost perfectly with transferrin after 20 minutes of internalization, and the colocalization remained very good. After 60 minutes, both proteins had a perinuclear distribution in many cells. However, although we saw some colocalization in this region, the two proteins also noticeably diverged from each other into separate perinuclear structures (Fig. 1.2C). We concluded that this decrease in colocalization at 60 minutes was likely due to the transferrin and the CTxB being sorted into two different pathways.

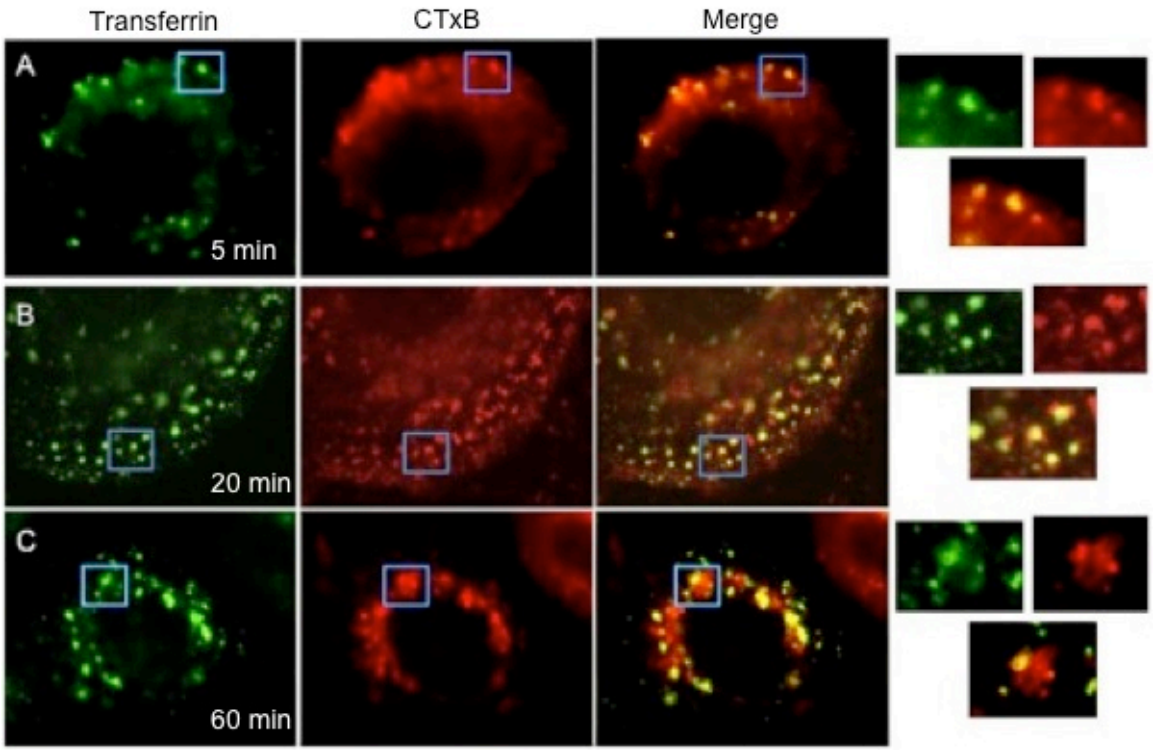

Figure 1.2. CTxB and transferrin colocalization in a time-dependent manner. CTxB is stained red while transferrin is green. A: after 5 minutes of internalization, B: after 20 minutes of internalization and C: after 60 minutes of internalization of CTxB (10 µg/mL) and transferrin (50 µg/mL). A total volume of 100 µL of CTxB and transferrin diluted in DMEM were applied to each dish and internalized at 37°C.

Unfortunately, we do not know whether caveolin-1 is present as a steady state at all times or if it is being internalized, and we cannot label it to determine which is the case due to the lack of an extracellular domain on the protein. Therefore, we internalized CTxB and expressed GFP-tagged caveolin-1 using transient transfection to try to determine whether CTxB labeled the same structures as caveolin-1. We observed that there was some colocalization after 5 minutes of internalization between CTxB and GFP-tagged caveolin-1, they appeared to colocalize well at 20 minutes, and at 60 minutes the colocalization was present to approximately the same extent as at 20 minutes (Fig. 1.3). However, we noticed that at 60 minutes, both CTxB and caveolin-1 accumulated in a perinuclear compartment in many cells (Fig. 1.3C). In contrast to the divergence of

CTxB and transferrin at this time, CTxB and caveolin-1 colocalized almost completely. Since this localization pattern is unusual for caveolin-1, which is normally stably associated with the plasma membrane, or cycles between there and caveosomes (Parton and Richards, 2003), we wanted to learn more about this perinuclear compartment and its function.

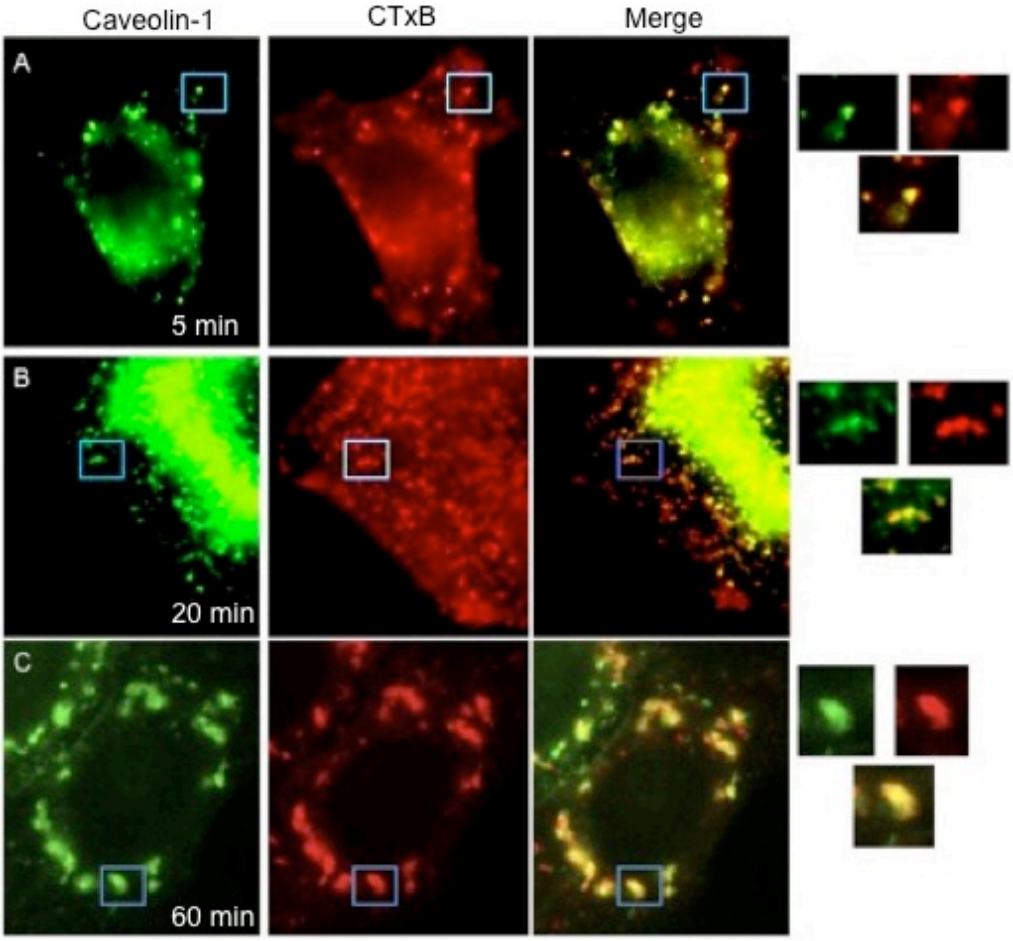

Figure 1.3. Caveolin-1 and CTxB colocalize in a time dependent manner. Caveolin-1 is stained green while CTxB is stained red. A: after 5 minutes of internalization, B: after 20 minutes of internalization and C: after 60 minutes of internalization of CTxB (10 µg/mL). Cells were transfected with 1 µg caveolin-1-GFP plasmid. One hundred microliters of CTxB diluted in DMEM was applied to each dish and internalized at 37°C.

Before focusing on this issue, though, we wanted to address one additional question. Since CTxB colocalized with both transferrin and caveolin-1 at each time

point to varying degrees, this raised the question of whether or not transferrin colocalized with caveolin-1 at any point. We checked this by internalizing transferrin for 5, 20 and 60 minutes and staining for caveolin-1 (Fig. 1.4). Although there was no observed colocalization after 5 minutes of internalization (Fig. 1.4A), caveolin-1 and transferrin colocalized well after 20 minutes of internalization, and there was some colocalization present after 60 minutes of internalization. The colocalization at 20 minutes was most likely due to both proteins being directed to early endosomes for sorting after internalization via different pathways, and then being sorted again for transport to different parts of the cells. These results agreed with previous findings which showed that the caveolin-1 and transferrin endocytosis pathways diverge after passing through early endosomes (Mundy et al., 2002). The difference in localization of caveolin-1 and CTxB compared to transferrin after 60 minutes of internalization indicates that the perinuclear compartment receives specific proteins, although the targeting/sorting mechanism is currently unknown.

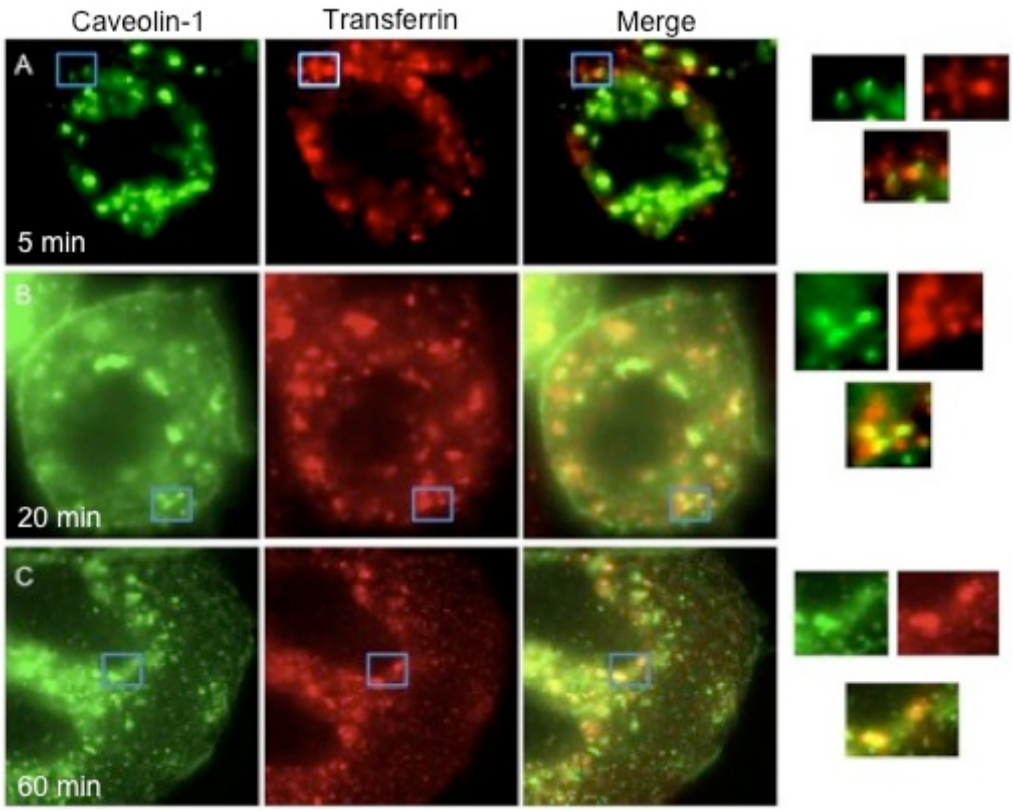

Figure 1.4. Caveolin-1 and transferrin colocalization in a time-dependent manner. Caveolin-1 is stained green while transferrin is red. A: after 5 minutes of internalization, B: after 20 minutes of internalization and C: after 60 minutes of internalization of transferrin (50 µg/mL). Cells were transfected with 1 µg caveolin-1-GFP plasmid. One hundred microliters of transferrin diluted in DMEM was applied to each dish and internalized at 37°C.

However, since CTxB colocalized with both transferrin and caveolin-1 at 60 minutes, we asked whether or not caveolin-1 affected CTxB transport in SKBr3 cells. To answer this question, we performed a triple label experiment in which we transfected SKBr3 cells with HA-tagged caveolin-1 and internalized both CTxB and transferrin for 5, 20 and 60 minutes (Fig. 1.5). We stained for caveolin-1 and looked for colocalization between all three markers. We saw some colocalization between both CTxB and either caveolin-1 or transferrin at 5 minutes in transfected cells, which indicated that CTxB was coming in via both caveolar endocytosis and clathrin-dependent endocytosis. At 20 minutes we saw significant colocalization between all three markers, most likely due to

their presence in early endosomes. At 60 minutes we observed that, in addition to colocalization between CTxB and caveolin-1, there was also colocalization between CTxB and transferrin, which indicated that cargos have to be sorted into the perinuclear compartment and that it was endocytic.

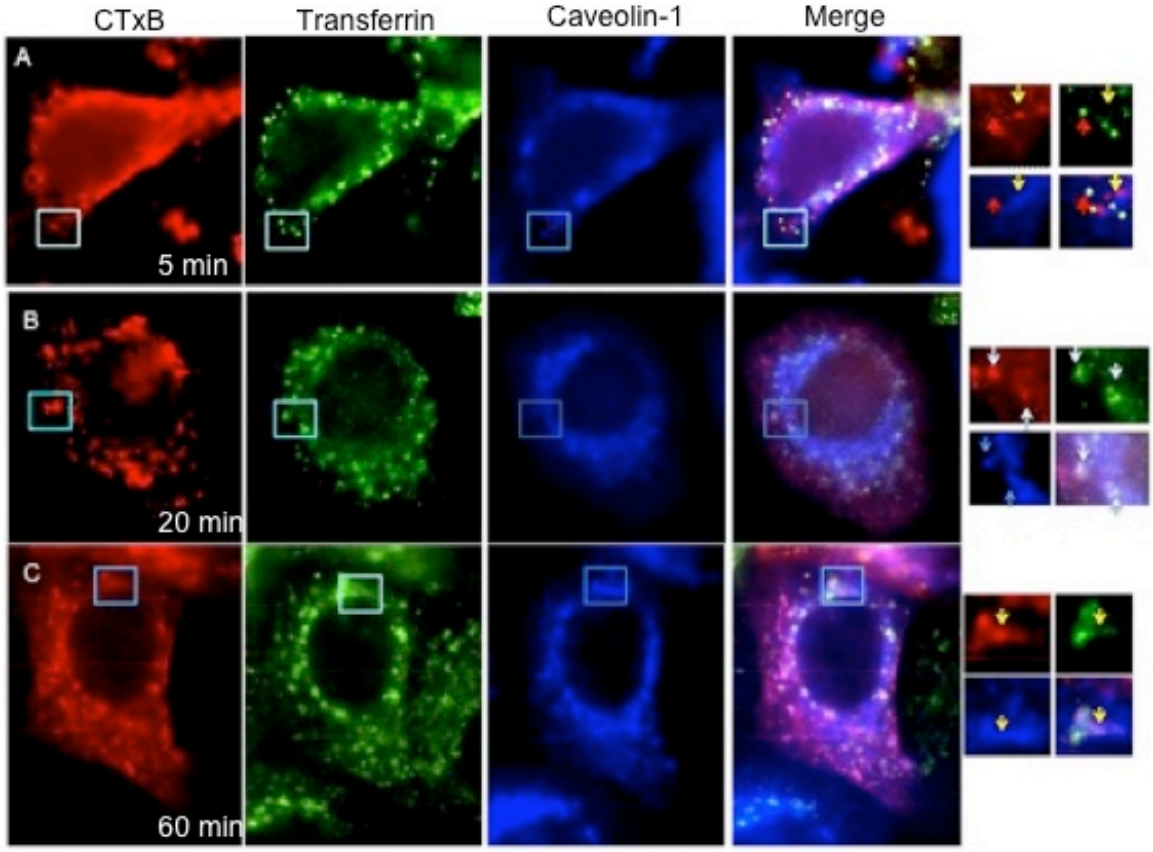

Figure 1.5. Colocalization of caveolin-1, CTxB and transferrin in a time-dependent manner. CTxB is stained red, transferrin is green, and transfected caveolin-1 is blue. A: after 5 minutes of internalization, B: after 20 minutes of internalization and C: after 60 minutes of internalization of CTxB (10 µg/mL) and transferrin (50 µg/mL). Red arrows indicate colocalization between CTxB and transferrin, yellow arrows indicate colocalization between CTxB and caveolin-1, white arrows indicate colocalization between all three proteins. Cells were transfected with 1 µg HA-tagged caveolin-1. One hundred microliters of CTxB and transferrin diluted in DMEM were applied to each dish and internalized at 37°C.

Characterization of the perinuclear compartment

To learn more about the perinuclear compartment, we internalized ruby red dextran into caveolin-1 transfected cells (Fig. 1.6) for 20 and 60 minutes. Ruby red

dextran is a fluid phase marker that is endocytosed non-specifically. We observed that the dextran colocalized well with caveolin-1 at 20 minutes in macropinosomes, but it didn't colocalize at all with caveolin-1 at 60 minutes. This seemed surprising, as any compartment labeled by CTxB must have been endocytic. However, since the dextran only labels compartments where there is a large volume: surface area ratio (such as large vesicles). For this reason, if the perinuclear compartment were composed of tubules and/or small vesicles, or if CtxB were transported through structures like this to access the perinuclear compartment, then the dextran might not be concentrated enough there to be detected. This result suggested that the perinuclear compartment may be composed of a network of small structures.

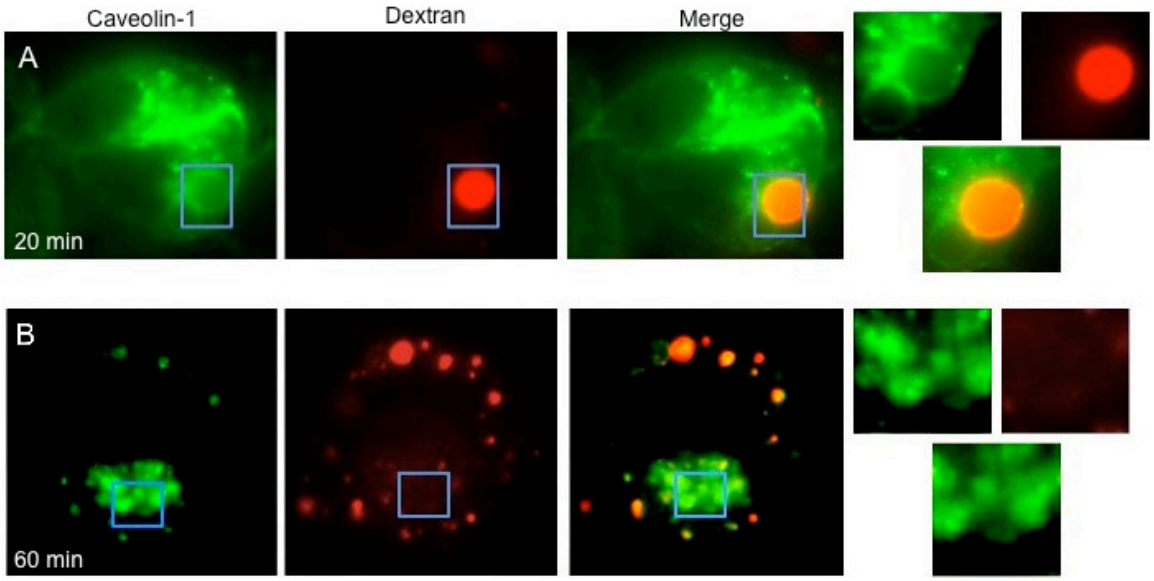

Figure 1.6. Colocalization of ruby red dextran (a fluid phase marker) with caveolin-1. A) After 20 minutes of internalization of ruby red dextran and B) after 60 minutes of internalization of ruby red dextran. Caveolin-1 is stained green and dextran is red. Cells were transfected with 1 µg GFP-tagged caveolin-1 and 1 mg/mL ruby red dextran was diluted in DMEM. One hundred microliters was applied to each dish and incubated at 37°C.

Since some endocytic pathways are cholesterol dependent, we used methyl-β-cyclodextrin (MBCD) to deplete the cells of cholesterol to try and discover whether

caveolin-1 localization, and by association caveolar endocytosis, was cholesterol-dependent (Fig. 1.7). MBCD removes cholesterol from cultured cells by forming soluble inclusion complexes that enhance the solubility of cholesterol in aqueous solution. We internalized ruby red dextran into caveolin-1 transfected cells for 20 minutes, and treated the cells with 10 mM MBCD for either 20 or 45 minutes. There was no difference between the control cells and the drug-treated cells, and caveolin-1 was still seen in the perinuclear compartment even after MBCD treatment, indicating that this sorting pathway is not completely cholesterol dependent. Large vacuoles were especially common after MBCD treatment (Fig. 1.7B). These were probably macropinosomes, as they could be labeled with internalized dextran.

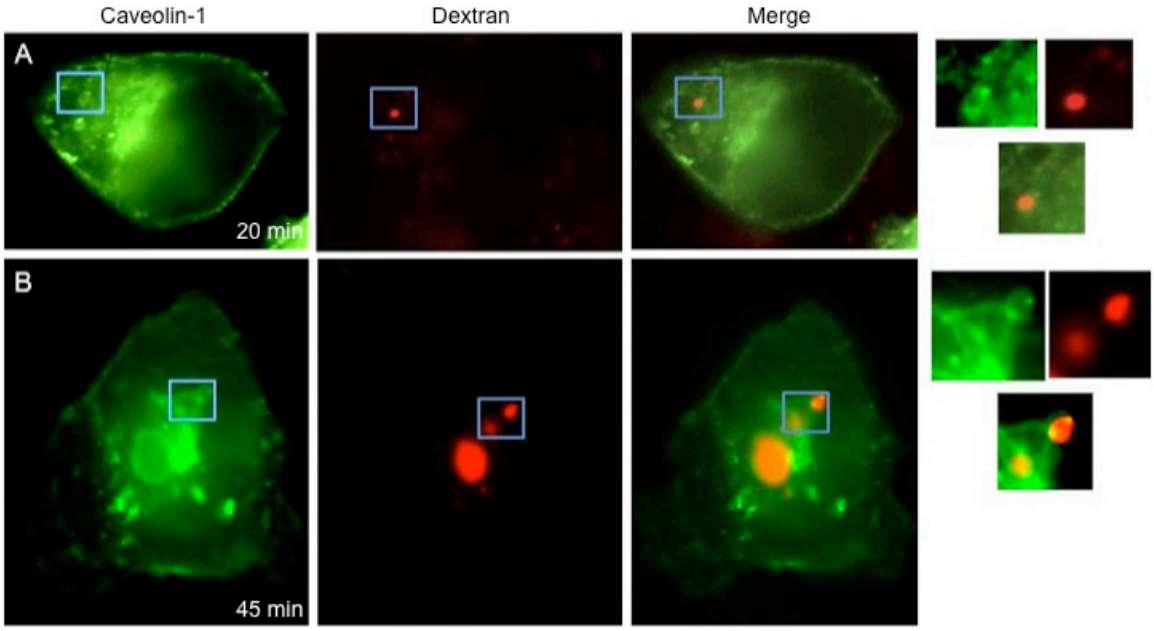

Figure 1.7. Effect MBCD on ruby red dextran and caveolin-1 colocalization. A) 20 minute treatment with MBCD coinciding with 20 minute ruby red dextran internalization. B) 25 minute treatment with MBCD followed by 20 minute treatment with MBCD coinciding with 20 minute ruby red dextran internalization. Cells were transfected with 1 µg GFP-tagged caveoliin-1 and 1 mg/mL ruby red dextran was diluted in DMEM. One hundred microliters was applied to each dish and incubated at 37°C.

Our next goal was to characterize the perinuclear compartment in which CTxB

and caveolin-1 colocalized further. A number of different structures are present in the perinuclear region of the cell, where they can be very close to each other and therefore are hard to distinguish from each other, but which fulfill different functions. For instance, the *trans*-Golgi network (TGN) and the endocytic recycling compartments can be very close together (Ghosh et al., 1998; Johnson et al., 1996). In some cells, the Golgi cisternae and the TGN are also so close that it's hard to distinguish them by immunofluorescence microscopy. Nonetheless, it is easier to distinguish the Golgi from the TGN in SKBr3 cells than in many other cell types. Thus, to try and determine whether the perinuclear compartment was part of the Golgi network, we stained three different Golgi markers (GM130, Galactosyl Transferase (GalTrans), and TGN46) and looked for any colocalization with either CTxB or caveolin-1 (Figs. 1.8 – 1.10). When we stained for either GM130 (Fig. 1.8A) or GalTrans (Fig. 1.9A) in caveolin-1 transfected cells, we saw virtually no colocalization between the proteins, although they were located in the same regions of the cell. However, when we internalized CTxB and stained for either GM130 (Fig. 1.8B) or GalTrans (Fig. 1.9B), we saw some cells, which had some colocalization, while other cells had no colocalization of the proteins. In addition, when we stained for TGN46 (a *trans*-Golgi network protein), although we saw some colocalization with both caveolin-1 (Fig. 1.10A) and CTxB (Fig. 1.10B), the structures labeled by the proteins appeared to occur more often as closely adjacent, possibly connected, structures. However, both proteins colocalized better with TGN46 than with the other Golgi markers. It was hard to determine whether these proteins were in the TGN, perhaps in a TGN subcompartment that overlapped only partially with TGN46.

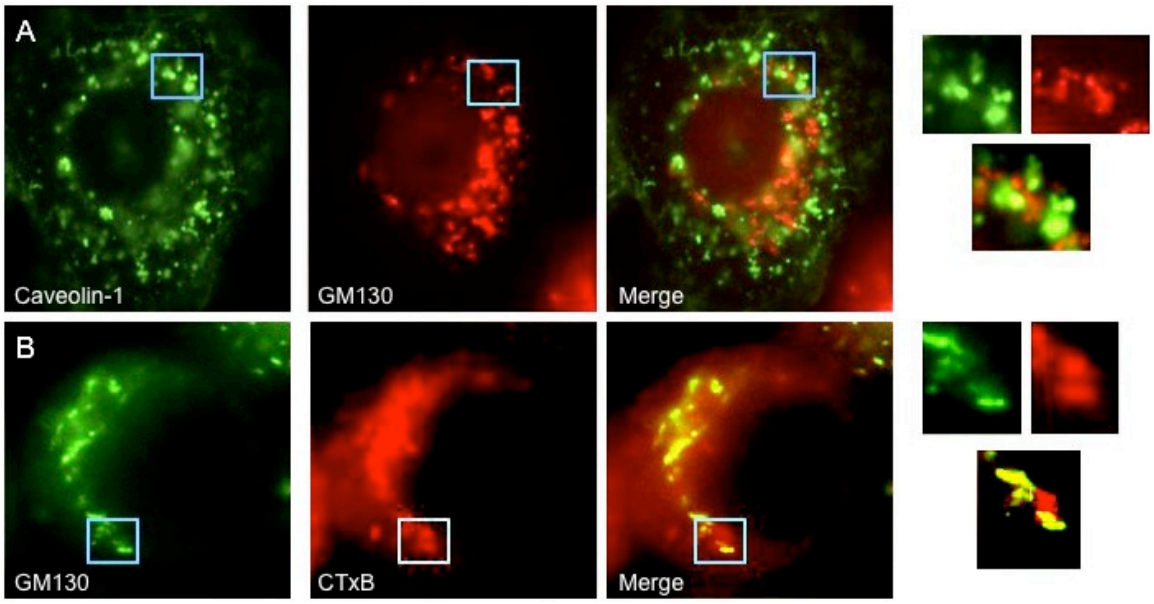

Figure 1.8. Colocalization of Caveolin-1 or CTxB with GM130, a Golgi marker. A) Caveolin-1 is stained green while GM130 is red. B) CTxB is stained red while GM130 is green. Cells were transfected with 1 µg GFP-labeled caveolin-1 or internalized with 10 µg/mL CTxB for 1hour. One hundred microliters of CTxB diluted in DMEM were applied and internalized at 37°C.

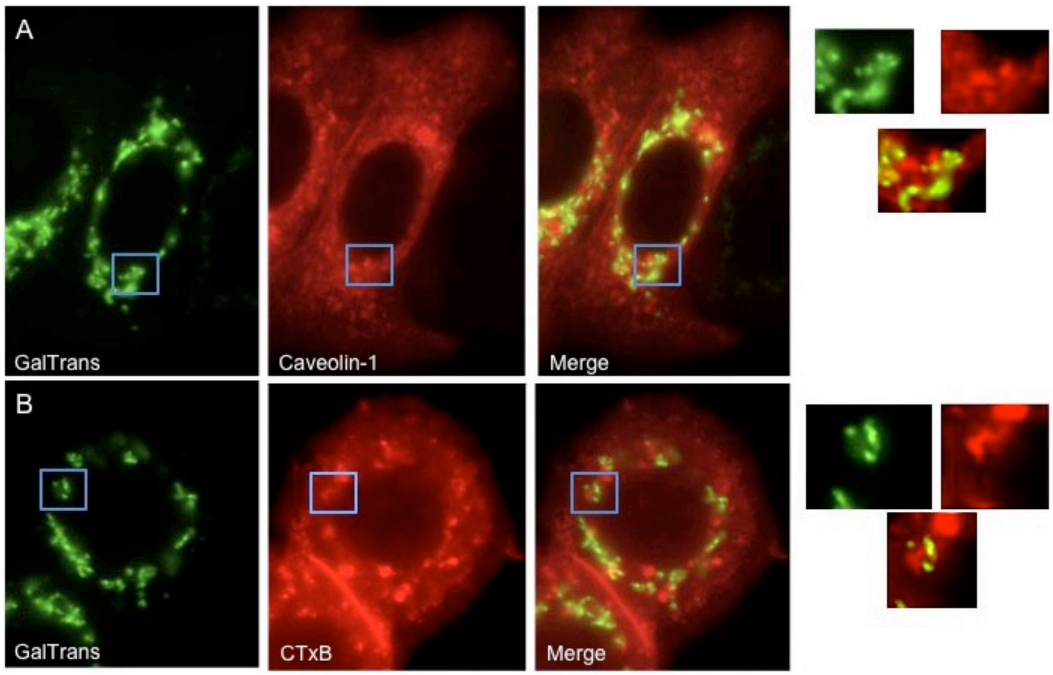

Figure 1.9. Colocalization of Caveolin-1 or CTxB with GalTrans, a Golgi marker. A) Caveolin-1 is stained red while GalTrans is green. B) CTxB is stained red while GalTrans is green. Cells were transfected with 1 µg YFP-labeled GalTrans and either 1 µg RPF-tagged caveolin-1 or internalized 10 µg/mL CTxB for 1hour. One hundred microliters of CTxB diluted in DMEM were applied and internalized at 37°C.

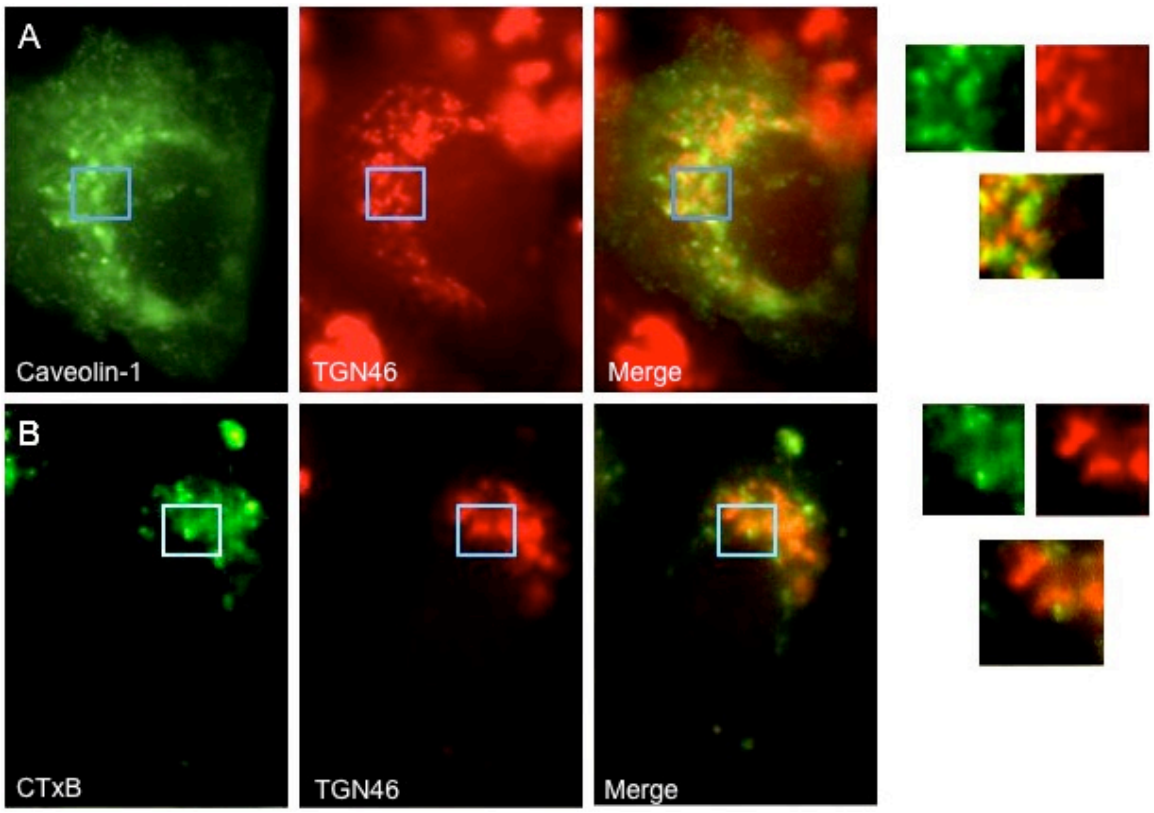

Figure 1.10. Colocalization of Caveolin-1 or CTxB with TGN46, a *trans*-Golgi network marker. A) Caveolin-1 is stained green while TGN46 is red. B) CTxB is stained green while TGN46 is red. Cells were transfected with 1 µg GFP-tagged caveolin-1 or internalized 10 µg/mL CTxB for 1hour. One hundred microliters of CTxB diluted in DMEM were applied and internalized at 37°C.

Since different compartments, including the TGN and endocytic recycling compartments, can be present in the perinuclear region of the cell, it may be difficult to tell them apart and thus the apparent colocalization or lack of colocalization of a protein with a marker of one of these compartments may be misleading. For this reason, although caveolin-1 and CTxB appeared to colocalize with each other, and both appeared to be close to the TGN, we wanted to use different treatments that might make it easier to tell the different compartments apart. One such treatment is brefeldin A (BFA) which is well-known to disrupt the Golgi. BFA initially causes the Golgi to form tubules, which disappear rapidly as they fuse with the ER, thus merging the Golgi membrane with the

ER membrane. In addition, BFA also causes the TGN and endosomes to form tubules, but less is known about this process than about the effect of BFA on the Golgi. However, in contrast to tubules originating from the Golgi, tubules originating from the TGN and endosomes are stable, and persist for hours in the presence of BFA. These tubules may also colocalize with each other.

We reasoned that BFA treatment might tell us whether the perinuclear pools of CTxB and caveolin-1 were in the TGN. If so, they should be present together with a TGN marker on tubules, which should be easier to distinguish from other compartments than is the compact perinuclear TGN in control cells. We internalized CTxB with BFA for 1 hour, and stained for either TGN46 or GM130 (Fig. 1.11A and B). We observed that, although TGN46 and CTxB both labeled tubules in BFA-treated cells, there was no colocalization between these proteins on the tubules. On the other hand, although the CTxB still formed tubules in the GM130-labeled cells, there were no GM130 positive tubules. These results suggested that the perinuclear compartment is structurally distinct from the TGN, but the two are very closely associated.

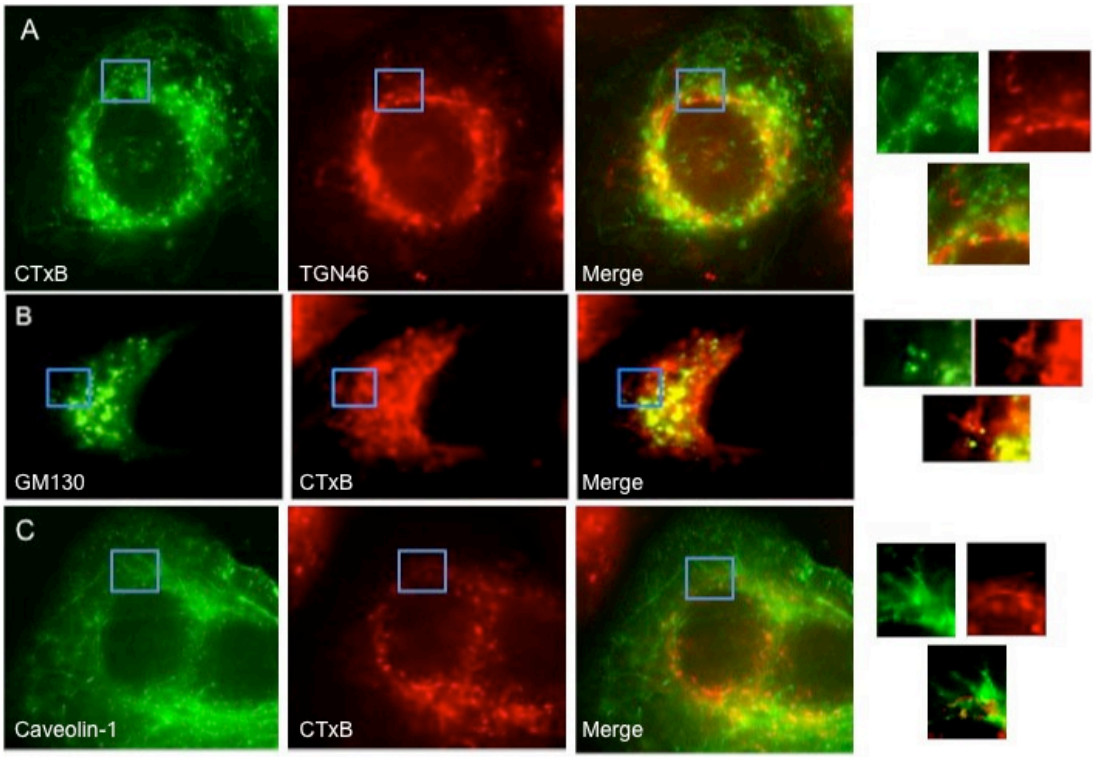

Figure 1.11. Effect of BFA on two different Golgi network markers (TGN46 and GM130), CTxB and caveolin-1. A) TGN46 is stained red while CTxB is stained green. B) GM130 is stained green while CTxB is stained red. C) Caveolin-1 is stained green while CTxB is stained red. Cells were transfected with 1 µg GFP-tagged caveolin-1 and/or internalized with 10 µg/mL CTxB for 1 hour. One hundred microliters of CTxB diluted in DMEM was applied to each dish and incubated at 37°C.

We also incubated caveolin-1 transfected cells with BFA and internalized CTxB for 1 hour (Fig. 1.11C). Surprisingly, we did not observe any tubular colocalization between the two proteins. We saw CTxB-positive tubules that were not labeled by caveolin-1 in the perinuclear region of most cells after BFA treatment. We also saw caveolin-1-positive tubules, which did not stain well for CTxB, in a few cells after BFA treatment. These tubules were usually closer to the plasma membrane than the CTxB-positive tubules. We had previously shown that, in a small subset of transfected SKBr3 cells, caveolin-1 forms tubules from the plasma membrane, which are likely still linked to the plasma membrane at one end and can be tens of microns long, extending deep into the cell (P. Verma et al., submitted for publication). We suspect that the caveolin-1-positive

tubules we saw in BFA-treated cells were the same as these tubules, and formed independently of BFA treatment. We do not know where the CTxB in the CTxB-positive tubules came from, although it was likely to originate from the perinuclear compartment. We do not know why caveolin-1 was not present on the CTxB-positive tubules. If CtxB and caveolin-1 were actually present in the same perinuclear compartment in control cells, BFA may have induced segregation of the two proteins, preventing caveolin-1 from entering the CTxB tubules. Alternatively there may have been two separate but very closely-associated perinuclear compartments. If so, only the CTxB containing-compartment could form tubules after BFA treatment.

Lastly, we asked whether or not the perinuclear compartment was involved in recycling. Previous studies have shown that myosin Vb regulates a recycling pathway, and that expression of the tail of myosin Vb alone results in a dominant negative phenotype and causes the affected proteins to accumulate together with the myosin Vb tail in a perinuclear localization pattern (Lapierre et al., 2001; Roland et al., 2007). These studies led us to ask whether the myosin Vb pathway was involved in caveolin-1 and/or CTxB recycling.

We expressed myosin Vb tail in SKBr3 cells, and either internalized CTxB for 1 hour (Fig. 1.12A) or co-expressed the myosin Vb tail with caveolin-1 (Fig. 1.12B). We noticed that myosin Vb colocalized well with caveolin-1 in discrete puncta. In some cases, most of the caveolin-1 in the cell was present in these structures, suggesting that it was trapped there by the myosin Vb tail. In contrast, CTxB did not colocalize at all with myosin Vb tail-positive puncta (Fig. 1.12A). Instead, it was present in amorphous perinuclear structures.

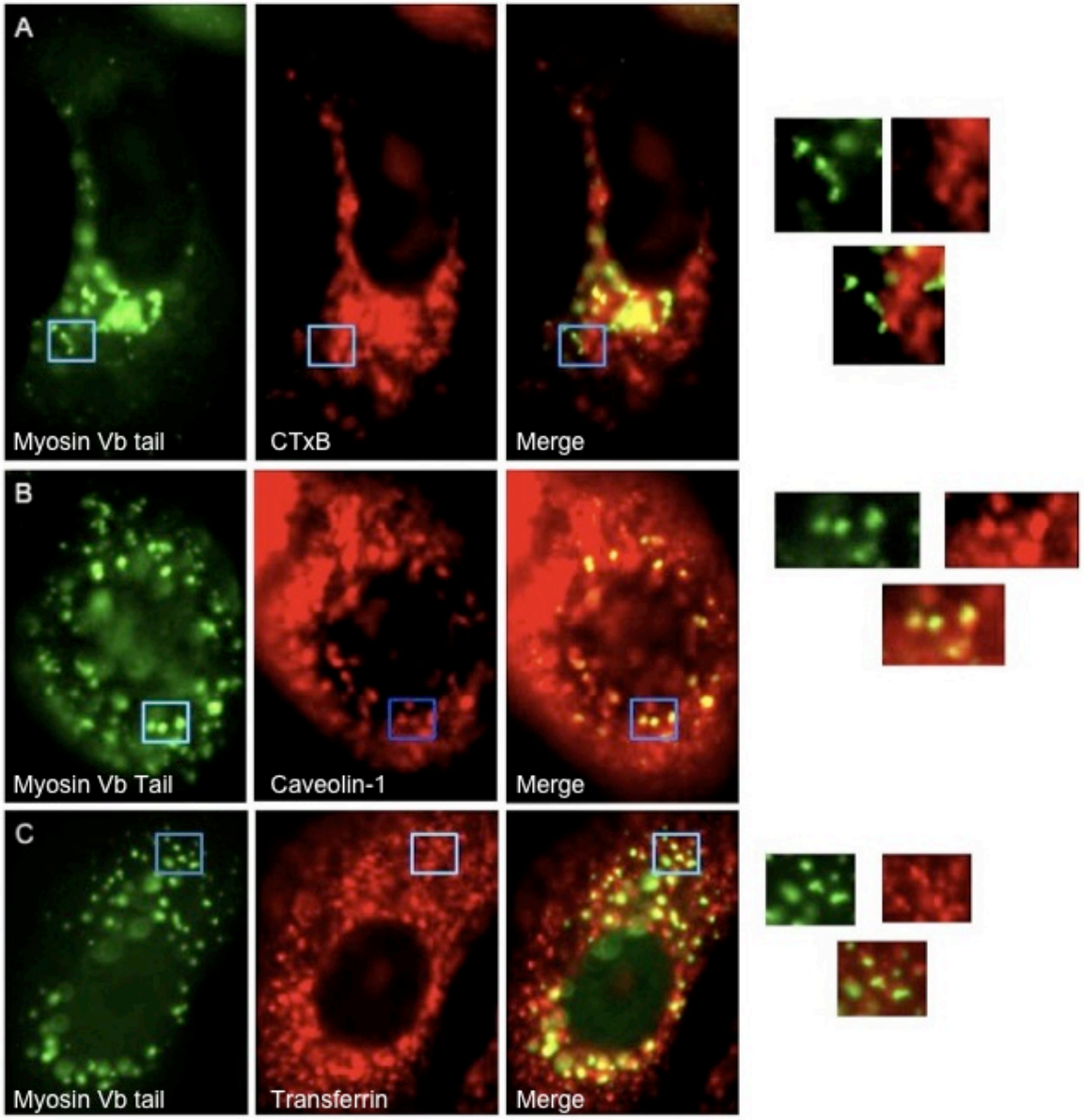

Figure 1.12. Colocalization of caveolin-1, CTxB or transferrin with Myosin Vb tail. A) Myosin Vb tail is stained green while CTxB is stained red. B) Myosin Vb tail is stained green while caveolin-1 is stained red. C) Myosin Vb tail is stained green while transferrin is stained red. Cells were transfected with 1 µg GFP-tagged myosin Vb tail and either 1 µg RFP-tagged caveolin-1 or internalized 50 µg/mL transferrin or 10 µg/mL CTxB diluted in DMEM. One hundred microliters were applied to each dish and incubated at 37°C for 1 hour.

We concluded that myosin Vb tail affected caveolin-1 differently from CTxB. The perinuclear localization of CTxB was not noticeably affected by myosin Vb tail, suggesting that the perinuclear CTxB-positive compartment was not a myosin Vb-

regulated recycling compartment. A pool of caveolin-1 may also have been present in the same myosin Vb-insensitive perinuclear compartment. In future studies, it would be interesting to perform triple-label studies, determining whether caveolin-1 and CTxB colocalized in amorphous, myosin Vb tail-negative perinuclear structures in myosin Vb-transfected cells. In addition, though, some caveolin-1 accumulated in myosin Vb-positive puncta. We can imagine two possible explanations of this result. First, caveolin-1 might have been sorted to a myosin Vb-regulated recycling pathway, separately from CTxB. Alternatively, the myosin Vb-positive puncta might have been on the secretory pathway. In epithelial cells, myosin Vb regulates TGN-to-plasma membrane transport as well as recycling. Caveolin-1 might have been trapped in this compartment on the way to the plasma membrane.

Finally, in agreement with previous work (Lapierre et al., 2001), we saw no colocalization between myosin Vb tail and transferrin (Fig. 1.12C). This confirmed the earlier report that transferrin recycles through a myosin Vb-dependent pathway.

Unlike CTxB, caveolin-1 might access the *trans*-Golgi network (TGN) by either of two routes: by endocytosis and retrograde transport, or during biosynthetic transport to the plasma membrane. Membrane proteins sometimes accumulate in the Golgi apparatus and/or TGN during transport to the cell surface, especially when over-expressed. However, it has been previously shown that, because caveolin-1 is a stable protein, a brief treatment with cycloheximide can clear caveolin-1 from the secretory pathway, without greatly affecting overall cellular levels of the protein (Ren et al., 2004). Therefore, in order to determine whether the perinuclear pool of caveolin-1 represented a protein pool that was in transit along the secretory pathway, we treated the cells with

cycloheximide for 1 or 3 hours, and internalized CTxB for the final hour of each condition (Fig. 1.13). This treatment should clear the secretory pathway. If perinuclear caveolin-1 were in transit to the plasma membrane, it should disappear during this time. However, we observed no real difference between the different conditions. This suggested that caveolin-1 reached the perinuclear compartment via an endocytic pathway, and not during biosynthetic transport to the plasma membrane.

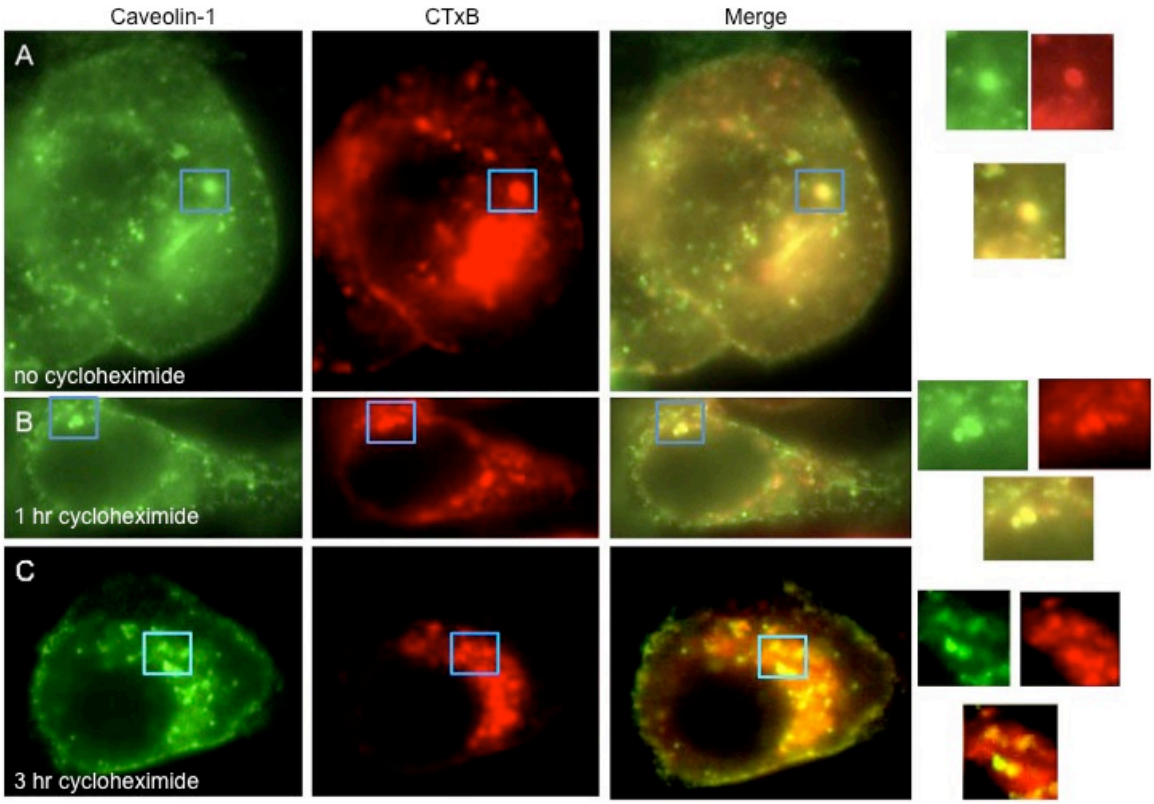

Figure 1.13. Effect of biosynthesis inhibition on the perinuclear compartment using cycloheximide. Caveolin-1 is stained green while CTxB is stained red. A) 1 hour internalization of CTxB without cycloheximide. B) 1 hour internalization of CTxB with 1 hour 100 µg/mL cycloheximide. C) 1 hour internalization of CTxB with 3 hours 100 µg/mL cycloheximide. Cells were transfected with 1 µg GFP –tagged caveolin-1. One hundred microliters of CTxB diluted in DMEM were applied to each dish and internalized at 37°C.

Discussion:

We investigated the trafficking pattern of caveolin-1 in SKBr3 cells and partially characterized a perinuclear compartment which exhibited an unusual caveolin-1 localization pattern. Since caveolin-1 does not contain an extra-cellular domain, here we used CTxB as a marker for caveolar endocytosis. Through internalization of CTxB and transferrin, our initial results showed that caveolin-1 is sent to early endosomes before being shipped to other parts of the cell. We also observed an unusual perinuclear localization pattern for caveolin-1 at long incubation times, and sought to learn more about this perinuclear compartment. It is possible that the relative rates of caveolin-1 trafficking have been altered in the course of the transformation of SKBr3 cells, since they have lost all caveolin-1 expression. If that is indeed the case, it is possible that this perinuclear localization is also present in normal cells, but that caveolin-1 is cleared from the perinuclear compartment too quickly to be detected. We confirmed that this compartment receives endocytic cargo through colocalization studies with CTxB, and cargos appear to be sorted into this compartment, since transferrin seems to be excluded from this compartment.

Since many structures, including the TGN/Golgi and endocytic recycling compartments, are found in the perinuclear region, we investigated whether this perinuclear compartment was associated with the TGN and/or Golgi. Since the perinuclear compartment was not labeled with any of the TGN/Golgi markers, and none of the CTxB, caveolin-1 and TGN/Golgi BFA-induced tubules colocalized, it is unlikely that this compartment is a part of the main TGN/Golgi, although the possibility that it is an unlabeled TGN subcompartment cannot be dismissed.

The perinuclear compartment may be part of either the endocytic pathway or located between the early endosomes and the TGN as part of retromer-based transport. CTxB may be transported from the early endosomes to the *trans*-Golgi network via this pathway, since a similar protein, Shiga toxin, has been shown to use retromer-based transport (Popoff et al., 2007). However, it is unclear with which pathway (recycling, or retromer-based transport, or both) this compartment is associated, and the precise location along the relevant pathway is unknown, although clearly the proteins are shipped to it after passing through early endosomes.

One possible function for this compartment was that it holds excess proteins from biosynthesis. Although previous studies observed that a 3 hour treatment with cycloheximide was sufficient to clear caveolin-1 from the secretory pathway (Ren et al., 2004), here the cycloheximide treatments negate the possible biosynthetic function of this compartment since treatment with cycloheximide did not affect the perinuclear localization pattern of caveolin-1 at all.

Another possible function is for this compartment to act in one or more recycling pathways. To investigate this possibility, we used a dominant negative form of myosin Vb (myosin Vb tail) to inhibit myosin Vb-dependent recycling. Although caveolin-1 partially colocalized with myosin Vb, it also stained an amorphous perinuclear compartment similar to that stained by CTxB. This partial colocalization may be due to the dominant negative myosin Vb tail inhibiting traffic between the TGN and the cell surface, thus trapping both CTxB and caveolin-1 in that region, but it also clearly affects caveolin-1 in a way that it does not affect CTxB. Unfortunately, the reason for this differential effect is currently unknown.

More studies are necessary in order to attempt to discover the function of this perinuclear compartment. One unanswered question is whether the myosin Vb tail-labeled puncta are biosynthetic or endocytic. In order to address this question, we would need to express a secreted protein, apically secreted if possible, and see if it stalled at some point along the pathway. We would also need to endocytose other proteins and observe their trafficking patterns relative to the perinuclear compartment and myosin Vb tail. Unfortunately, GFP cannot be acid washed, so internal signals are more difficult to detect. These studies, in addition to future work fully characterizing the perinuclear compartment, can provide new insights into the fascinating and under-explored topic of caveolin-1 trafficking, and may provide new avenues in the treatment of genetic disorders including cancer.

References:

Alberts, B., A. Johnson, J. Lews, M. Raff, K. Roberts, and P. Walter. 2007. Molecular Biology of the Cell. Garland Science, New York, NY.

Brodsky, F.M., C.-Y. Chen, C. Knuehl, M.C. Towler, and D.E. Wakeham. 2001. Biological basket weaving: formation and function of clathrin-coated vesicles. *Annual Review of Cell and Developmental Biology*. 17:517-568.

Conner, S.D., and S.L. Schmid. 2003. Regulated portals of entry into the cell. *Nature*. 422:37-44.

Doherty, G.J., and H.T. McMahon. 2009. Mechanisms of endocytosis. *Annual Review of Biochemistry*. 78.

Ghosh, R.N., W.G. Mallet, T.T. Soe, T.E. McGraw, and F.R. Maxfield. 1998. An endocytosed TGN38 chimeric protein is delivered to the TGN after trafficking through the endocytic recycling compartment in CHO Cells. *J. Cell Biol.* 142:923-936.

Guillot, F.L., K.L. Audus, and T.J. Raub. 1990. Fluid-phase endocytosis by primary cultures of bovine brain microvessel endothelial cell monolayers. *Microvascular Research*. 39:1-14.

Hazes, B., and R.J. Read. 1997. Accumulating evidence suggests that several AB-toxins subvert the endoplasmic reticulum-associated protein degradation pathway to enter target cells. *Biochemistry*. 36:11051-11054.

Johannes, L., and V. Popoff. 2008. Tracing the retrograde route in protein trafficking. *Cell*. 135:1175-1187.

Johnson, A., R. Ghosh, K. Dunn, R. Garippa, J. Park, S. Mayor, F. Maxfield, and T. McGraw. 1996. Transferrin receptor containing the SDYQRL motif of TGN38 causes a reorganization of the recycling compartment but is not targeted to the TGN. *J. Cell Biol.* 135:1749-1762.

Lencer, W.I., and B. Tsai. 2003. The intracellular voyage of cholera toxin: going retro. *Trends in Biochemical Sciences*. 28:639-645.

Majoul, I., K. Sohn, F.T. Wieland, R. Pepperkok, M. Pizza, J. Hillemann, and H.-D. Soling. 1998. KDEL receptor (Erd2p)-mediated retrograde transport of the cholera toxin A subunit from the Golgi involves COPI, p23, and the COOH terminus of Erd2p. *J. Cell Biol.* 143:601-612.

Majoul, I.V., P.I.H. Bastiaens, and H.-D. Soling. 1996. Transport of an external Lys-Asp-Glu-Leu (KDEL) protein from the plasma membrane to the endoplasmic reticulum: studies with cholera toxin in Vero cells. *J. Cell Biol.* 133:777.

Mundy, D.I., T. Machleidt, Y.-s. Ying, R.G.W. Anderson, and G.S. Bloom. 2002. Dual control of caveolar membrane traffic by microtubules and the actin cytoskeleton. *J Cell Sci*. 115:4327-4339.

Nichols, B. 2003. Caveosomes and endocytosis of lipid rafts. *J Cell Sci*. 116:4707-4714.

Parton, R.G., and A.A. Richards. 2003. Lipid rafts and caveolae as portals for endocytosis: new insights and common mechanisms. *Traffic*. 4:724-738.

Parton, R.G., and K. Simons. 2007. The multiple faces of caveolae. *Nat Rev Mol Cell Biol*. 8:185-194.

Pelkmans, L., T. B¸rli, M. Zerial, and A. Helenius. 2004. Caveolin-stabilized membrane domains as multifunctional transport and sorting devices in endocytic membrane traffic. *Cell*. 118:767-780.

Pelkmans, L., and M. Zerial. 2005. Kinase-regulated quantal assemblies and kiss-and-run recycling of caveolae. *Nature*. 436:128-133.

Popoff, V., G.A. Mardones, D. Tenza, R. Rojas, C. Lamaze, J.S. Bonifacino, G. Raposo, and L. Johannes. 2007. The retromer complex and clathrin define an early endosomal retrograde exit site. *J Cell Sci*. 120:2022-2031.

Ren, X., A.G. Ostermeyer, L.T. Ramcharan, Y. Zeng, D.M. Lublin, and D.A. Brown. 2004. Conformational defects slow Golgi exit, block oligomerization, and reduce raft affinity of caveolin-1 mutant proteins. *Mol. Biol. Cell*. 15:4556-4567.

Richards, A.A., E. Stang, R. Pepperkok, and R.G. Parton. 2002. Inhibitors of COP-mediated transport and cholera toxin action inhibit simian virus 40 infection. *Mol. Biol. Cell*. 13:1750-1764.

Ridley, A.J. 2001. Rho proteins: linking signaling with membrane trafficking. *Traffic*. 2:303-310.

Rothberg, K.G., J.E. Heuser, W.C. Donzell, Y.-S. Ying, J.R. Glenney, and R.G.W. Anderson. 1992. Caveolin, a protein component of caveolae membrane coats. *Cell*. 68:673-682.

Sandvig, K., and B. van Deurs. 2002. Membrane traffic exploited by protein toxins. *Annual Review of Cell and Developmental Biology*. 18:1-24.

Sorkin, A., and L.K. Goh. 2008. Endocytosis and intracellular trafficking of ErbBs. *Exp Cell Res*. 314:3093-3106.

Tagawa, A., A. Mezzacasa, A. Hayer, A. Longatti, L. Pelkmans, and A. Helenius. 2005. Assembly and trafficking of caveolar domains in the cell: caveolae as stable, cargo-triggered, vesicular transporters. *J. Cell Biol.* 170:769-779.

Thomas, C.M., and E.J. Smart. 2008. Caveolae structure and function. *Journal of Cellular and Molecular Medicine*. 12:796-809.

Thorn, H., K.G. Stenkula, M. Karlsson, U. Ortegren, F.H. Nystrom, J. Gustavsson, and P. Stralfors. 2003. Cell surface orifices of caveolae and localization of caveolin to the necks of caveolae in adipocytes. *Mol. Biol. Cell*. 14:3967-3976.

Tsai, B., Y. Ye, and T.A. Rapoport. 2002. Retro-translocation of proteins from the endoplasmic reticulum into the cytosol. *Nat Rev Mol Cell Biol*. 3:246-255.

Xie, Z., X. Zeng, T. Waldman, and R.I. Glazer. 2003. Transformation of mammary epithelial cells by 3-phosphoinositide-dependent protein kinase-1 activates {beta}-catenin and c-Myc, and down-regulates caveolin-1. *Cancer Res*. 63:5370-5375.

Chapter 2: The Effect of Varying Bilayer Thickness on Caveolin-1 Hydrophobic Domain Topology in Model Membranes

Introduction:

Caveolin-1 is a 22 kDa protein that contains a single hydrophobic region that is 33 amino acid residues long. It has previously been shown that when caveolin-1 is associated with membranes, both the C- and N-termini are on the same side of the membrane with the hydrophobic region inserted into the membrane (Uittenbogaard and Smart, 2000). However, the conformation of the hydrophobic region, and how its conformation changes in response to cholesterol, is unknown. Therefore, we decided to make a peptide corresponding to the hydrophobic domain of caveolin-1 in order to study its topology in model membranes.

We believe that there are two possible conformations that the caveolin-1 hydrophobic domain may adopt: 1) it may form a hairpin loop in the membrane, or 2) it may lie parallel to the plane of the membrane. One of these two conformations is believed to result in caveolin-1 inducing curvature in a membrane. The two main mechanisms by which proteins induce membrane curvature are described in the following section.

Protein-induced curvature

Membrane bilayers prefer to be flat, but in cells, proteins interact with bilayers to induce curvature, which is how the various organelles achieve their characteristic shapes (Bonifacino and Lippincott-Schwartz, 2003; Polishchuk et al., 2000; Zimmerberg and Kozlov, 2006). Proteins that bind to the surface of a membrane can induce membrane

curvature through several different, but not exclusive, mechanisms. The two main mechanisms are scaffolding and bilayer-coupling (Zimmerberg and Kozlov, 2006). The scaffold mechanism assumes that certain proteins function as scaffolds, which impose the intrinsic curvature of the protein onto the lipid bilayer (Farsad and Camilli, 2003). This type of protein must satisfy several criteria in order to bend the local membrane. The protein's intrinsic shape must enable it to expose a curved surface to interact with the lipid bilayer, the protein must be intrinsically stiff enough to successfully counteract the bilayer's tendency to relax to its normal state of spontaneous curvature, and the protein must have enough affinity for the polar lipid head-groups to force the bilayer to fit to the shape of the protein (Zimmerberg and Kozlov, 2006) (Fig. 2.1A).

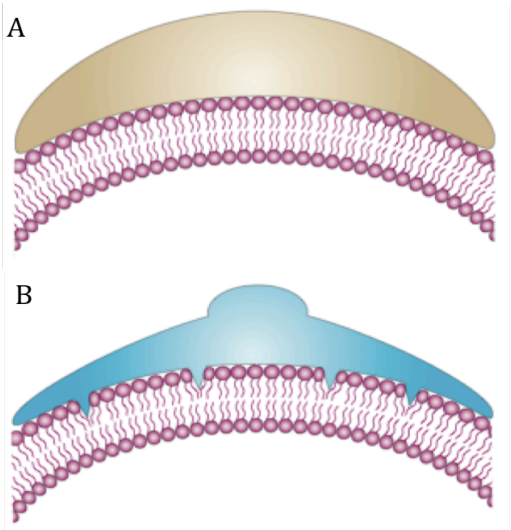

Fig. 2.1. The two primary mechanisms of protein-induced curvature. A) The scaffolding mechanism where the protein induces its curvature onto the native membrane. The brown structure represents a protein attached to the membrane. This protein is intrinsically curved and is imposing that curvature on the associated membrane. B) The bilayer-coupling mechanism where the protein inserts one or more moieties into one layer of the bilayer, thereby inducing curvature in the native membrane. The blue structure represents a protein attached to the membrane, and the little blue protrusions represent the protein's amphipathic helices. The protein inserts these helices into one leaflet of the bilayer, thereby causing the membrane to curve due to the resulting difference in area between the two leaflets. Source: (Zimmerberg and Kozlov, 2006).

The bilayer-coupling mechanism is based on the local deformation of membranes, which occurs in response to the insertion of protein regions (generally amphipathic) into the bilayer. As shown by the blue protrusions in Fig. 2.1B, when a portion of a protein is inserted into only one layer of a bilayer, it takes on the role of a wedge that causes a local monolayer deformation, thus resulting in curvature (Zimmerberg and Kozlov, 2006). Epsin, for example, has been shown to induce membrane curvature by inserting its ENTH (epsin N-terminal homology) domain, which consists of an amphipathic helix, into the membrane bilayer (Ford et al., 2002). In addition, although most proteins containing a BAR domain act as scaffolds, some proteins that contain a BAR domain also have amphipathic helices and have been shown to mediate membrane curvature through bilayer coupling (Gallop and McMahon, 2005; Peter et al., 2004). Furthermore, the reticulon family of proteins also may employ a combination of bilayer coupling and scaffolding in order to induce membrane curvature (Hu et al., 2008; Voeltz et al., 2006). It seems likely that, since caveolin-1 contains a single helical hydrophobic region, it would induce curvature via the bilayer-coupling mechanism, rather than through the scaffolding mechanism.

Since caveolin-1 may have two different alternate conformations, it may be able to interact with membranes in two different ways. One of these conformations may result in membrane curvature while the other may not. Other peptides have been shown to change the conformation in response to changes in pH (Caputo and London, 2004), and we attempted to discover whether the caveolin-1 peptide would change conformation in response to changes in bilayer thickness. Here we investigated the behavior of a caveolin-1 peptide, which contains the hydrophobic region of the full-length protein, in

synthetic model membranes. Using different membrane thicknesses and different quenchers we attempted to discover how these factors affect caveolin-1 position and orientation in model membranes, and thereby extrapolate to its conformation and behavior *in vivo*.

We collected our data using Trp fluorescence, which has been shown to be a good indicator of the relative position of Trp within a bilayer (Shahidullah and London, 2008). The Trp's maximum wavelength of emission fluorescence (λ_{max}) indicates how deeply the Trp is embedded in the membrane. The deeper the Trp is, the more blue-shifted the λ_{max} would be relative to the peptide in water while the shallower the Trp the more red-shifted the λ_{max} would be relative to the peptide in water.

Methods and Materials:

Materials

The mutant caveolin-1 peptide (Acetyl-DKDKDRLLSALFGIPMALIWGIYFAI-LSFLHIYAVVPAIKDDKKK-amide) was obtained from the Yale W. M. Keck Proteomics facility. This is identical to the hydrophobic domain of human caveolin-1 (RLLSALFGIPMALIWGIYFAILSFLHIWAVVPCIK; with the basic residues at each end of the domain included) except for the following changes, described briefly here and detailed in the Results section. First, charged residues were added to each end of the peptide to improve solubility and help the peptide achieve the correct topology in bilayers. Second, the second Trp in the native sequence was changed to Tyr, leaving only one Trp residue. Third, the Cys near the end of the hydrophobic domain, which is palmitoylated in vivo, was changed to Ala to facilitate synthesis and purification. Stock solutions of the lipids (14.39 mM DMoPC (dimyristoleoyl phosphatidylcholine, containing mono-unsaturated 14-carbon acyl chains), 51.78 mM DPOPC (dipalmitoleoyl phosphatidylcholine, containing mono-unsaturated 16-carbon acyl chains), 21.58 mM DOPC (dioleoyl phosphatidylcholine, containing mono-unsaturated 18-carbon acyl chains), 11.64 mM DiEPC (dieicosanoyl phosphatidylcholine, containing mono-unsaturated 20-carbon acyl chains), 25.12 mM DEuPC (dierucoyl phosphatidylcholine, containing mono-unsaturated 22-carbon acyl chains) and 27.3 mM DNPC (dinervonoyl phosphatidylcholine, containing mono-unsaturated 24-carbon acyl chains)) were made in chloroform. Since DNPC is close to its liquid disordered (L_d) to gel freezing point at room temperature, in order to form L_d DNPC-based vesicles, we mixed 66% DNPC with 33% DEuPC to obtain vesicles at room temperature with slightly thinner membranes

(23.3 carbons on average, instead of 24 carbons). Two quenchers were used, 10-DN (10-doxylnonadecane) (stock concentration of 7.58 mM, in chloroform), which quenches fluorescence from residues buried within the membrane and acrylamide (stock concentration of 4.0 M, in water), which quenches fluorescence from residues exposed to the aqueous buffer.

Purification

1.2-1.5 mg of the peptide was dissolved in 750 µL HPLC (high performance liquid chromatography) Buffer A (H_2O, 0.5% TFA (trifluoroacetic acid)) and 750 µL HPLC Buffer B (60% isopropanol, 40% acetonitrile, 0.5% TFA) and the solution was vortexed until no peptide particles could be seen. The sample was separated on a C4 column using a Dynamax HPLC system. 400 µL of the protein was loaded into the injector, and passed through the column in 50% Buffer A/50% Buffer B at a flow rate of 0.4 mL/min. The peptide was eluted by using a gradient that increased the concentration of Buffer B from 50% to 100% over a period of 90 minutes. All fractions corresponding to the major peaks on the data trace were collected and mass spectrometry was used to verify which fraction contained the peptide. In subsequent samples the fraction containing the peptide, which eluted at 38-41 minutes, was collected.

Vesicle formation

Ethanol dilution vesicles were formed by combining the lipids (final concentration of 500 µM) with the peptide (final concentration of 2 µM), cholesterol (accounting for 30 mol% of the lipid concentration) and quenchers as appropriate. The samples were dried using liquid nitrogen for five minutes and then by high vacuum for

one hour. The samples were then resuspended in 10 μL ethanol, vortexed, and 790 μL phosphate buffered saline (PBS) (pH 7.4) was added.

Fluorescence

The fluorescence of the single tryptophan present in the peptide was measured using a Fluordog fluorimeter. The excitation wavelength was set to 280 nm, and a fluorescence emission spectrum was taken between 300 and 370 nm. The wavelength of maximum fluorescence (λ_{max}) was determined to be the wavelength at which the fluorescence intensity was the greatest. The spectrum of the appropriate control was subtracted from each peptide sample to obtain the corrected peptide spectrum, which was used in the analysis. All experiments were performed in triplicate.

Fluorescence intensities were also measured using an excitation wavelength of 280 nm and fluorescence was measured at 330 nm for the 10-DN experiments. Sixteen mol% of 7.58mM 10-DN was added to 84 mol% of either DMoPC or DEuPC, for a total lipid+10-DN concentration of 500μM, prior to forming ethanol dilution vesicles as previously stated. For the acrylamide experiments, an excitation wavelength of 295 nm was used and fluorescence was measured at 340 nm. Fifty μL 4.0M acrylamide was added to the appropriate samples after vesicle formation, resulting in a total volume of 850 μL, instead of the standard 800 μL. Samples were run in triplicate and counts per second over a period of ten seconds were averaged. Data were normalized such that the control fluorescence had a value of one and the quenching ratio was measured as an x-fold increase or decrease relative to the control.

Results:

The native sequence of the caveolin-1 hydrophobic domain contains two conserved Trps (Trp1 and Trp2). Trp1 was conveniently located near the center of the peptide, where we predicted that it would be near the surface of the membrane if the peptide adopted a hairpin structure, perhaps buried within the bilayer if the peptide adopted a conformation that was parallel to the plane of the bilayer. These different positions would be distinguishable by changes in the maximum wavelength of emission fluorescence (λ_{max}) and by diferences in the accessibility to different quenchers. Trp2, on the hand, was located roughly three-quarters of the way along the sequence. In this position, it was expected that Trp 2 would be buried within the membrane regardless of which conformation the peptide adopted. Therefore the Trp2 was mutated to an alanine, in order to be certain all fluorescence was due to Trp1. Since it is known that caveolin-1 does not form a transmembrane conformation *in vivo* (Tagawa et al., 2005), we also added a combination of six Lys and Asp to each end of the peptide in an attempt to prevent it from forming the unwanted transmembrane conformation when it was added to pre-formed vesicles.

Since it is known that cholesterol depletion affects caveolae structure, we suspected that cholesterol may affect the structure of caveolin-1. However, we did not know how this occurred. One effect of cholesterol is to thicken membranes, and for this reason it is possible that the different conformations of caveolin-1 that may exist in the plasma membrane with and without cholesterol may simply reflect bilayer thickness, rather than a specific effect of cholesterol. Therefore, we wanted to determine whether or not caveolin-1 conformation was dependent on the thickness of the membrane bilayer

into which it had inserted and/or lipid composition since caveolae flatten out in cholesterol-depleted membranes. For this reason, we first studied the effects of different lipid compositions on Trp1 fluorescence of the caveolin-1 peptide in a simple system. A series of vesicles were made from phospholipids that differ in the length of their acyl chains, so that the vesicles would differ in their bilayer thickness.

We began by asking whether the λ_{max} of Trp1 would be different when added to vesicles of different thickness. If so, it would show that bilayer thickness affected peptide conformation. We first created a curve using six different lipids to determine whether Trp1 fluorescence would respond to changes in membrane thickness. In this experiment, for convenience, the peptide was mixed with the lipids before vesicle formation. For this reason, we did not know whether both ends of the peptide would be on the same side of the bilayer, mimicking the situation *in vivo*, or whether the peptide would adopt a transmembrane conformation during vesicle formation. We found that the λ_{max} increased, becoming more red-shifted, with increasing bilayer thickness. That is, in 14-carbon DMoPC vesicles the λ_{max} was about 336. The λ_{max} increased approximately linearly up to 20-carbon DiEPC vesicles, to about 346, after which the λ_{max} increased more slowly, to about 347 in 24-carbon DEuPC vesicles (Fig. 2.2). For comparison, expected λ_{max} values in various environments are displayed in Table 2.1. These range from a very red-shifted λ_{max} for 345 in water to 315-320 in the center of the bilayer. This result indicated that the thickness of the bilayer affected peptide conformation and/or disposition in the bilayer. In DMoPC ($\lambda_{max} \approx 336$), Trp1 appeared to be located in the border region of the membrane. Oddly, in DEuPC bilayers ($\lambda_{max} \approx 347$) the Trp1 λ_{max} was even more red-shifted than in water ($\lambda_{max} \approx 345$), and we currently do not have an

explanation for this surprising result. Of note is the fact that there are no λ_{max} values corresponding to a deeply buried peptide. This lack was expected since both of the expected caveolin-1 hydrophobic region conformations result in a relatively shallow Trp1 placement. In particular, the hairpin conformation would place Trp1 in the border region. We selected three representative lipids (DMoPC, DOPC and DEuPC) for use in later studies using thin, intermediate and thick membranes.

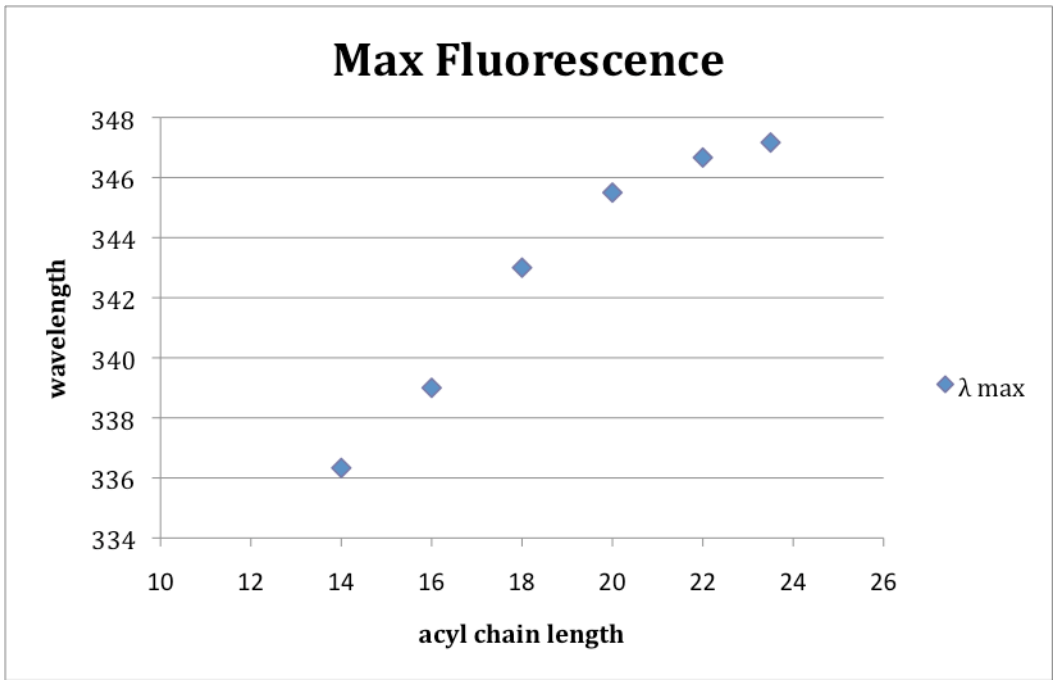

Figure 2.2. Graph of the λ_{max} of the tryptophan in the caveolin-1 peptide when in membrane bilayers of different thickness. The λ_{max} is decreased (less red-shifted) in thinner bilayers than in thicker bilayers. Lipids used were DMoPC (14 C), DPOPC (16 C), DOPC (18 C), DiEPC (20 C), DEuPC (22 C) and 66% DNPC + 33% DEuPC (~23 C)

Peptide Environment	Approximate λ_{max}
Aqueous	345
Bilayer border	336
Mid-bilayer	330
Bilayer center	315-320

Table 2.1. Table showing the approximate λ_{max} values generally obtained for Trp in different environments. The λ_{max} is generally most red-shifted in aqueous buffer, where there are no membrane bilayers present. A Trp located at the bilayer border is partially embedded in the bilayer, but still has access to the aqueous buffer. The λ_{max} of a Trp embedded in the center of the bilayer will be the least red-shifted.

We next performed a control experiment to determine whether the peptide formed the transmembrane conformation when the peptide was present with the lipids during vesicle formation. In order to do this, we compared two different samples. In one, we pre-mixed the peptide with the lipids before forming vesicles. In the other, we added it after the vesicles had been formed, preventing the formation of a transmembrane span, in the other sample. We then examined the λ_{max} in the two samples, to determine whether Trp1 was present in the same position in both. We performed this comparison in vesicles of three different lipid compositions: DMoPC, DOPC, and DEuPC. There was no significant difference between the two sets of data (Table 2.2), so the peptide was presumed to form the biologically relevant conformation with both termini on the same side of the bilayer even when mixed with the lipids prior to vesicle formation. If the peptide had formed the transmembrane conformation when pre-mixed with the lipids, we assumed that the λ_{max} would have remained relatively unaffected by the changes in membrane thickness when pre-mixed with the lipids.

Lipid Composition	Pre-mixed lipid + peptide λ_{max}	Peptide + preformed vesicles λ_{max}
DMoPC	336.3 ± 0.5 nm	337 ± 0 nm
DOPC	343 ± 0.7 nm	343.3 ± 1 nm
DEuPC	346.6 ± 1 nm	346.7 ± 0.3 nm
In Aqueous Buffer	342 ± 0.5 nm	

Table 2.2. The conformation of the caveolin-1 peptide is unlikely to be transmembraneous. As shown, the λ_{Max}s of pre-mixing the peptide with the lipids are very similar to the λ_{Max}s of adding the peptide to pre-formed vesicles. It is therefore assumed that the peptide is inserted into the membrane with both termini on the same side of the membrane.

As previously shown in Fig. 2.1, the λ_{max} increased as the length of the lipid chains increased. Since caveolae flatten out in cholesterol-depleted membranes *in vivo*, we asked whether adding cholesterol to model membranes affected the tryptophan λ_{max} in any way. We observed that the addition of cholesterol did not result in a significant change in λ_{max} in any vesicles (Table 2.3). However, we did not know whether or not cholesterol significantly changed the thickness of these membrane bilayers.

Lipid composition	Lipid + Peptide λ_{Max}	Lipid + Peptide + Cholesterol λ_{Max}
DMoPC	335.8 ± 0.5 nm	338 ± 1.5 nm
DOPC	340.5 ± 0.7 nm	341.3 ± 2 nm
DEuPC	346.5 ± 1 nm	345 ± 1 nm

Table 2.3. λ_{Max} of the caveolin-1 peptide tryptophan changes due to differences in the length of the lipid acyl chains, and the presence or absence of cholesterol. In DMoPC, which only has 14 carbons, the λ_{Max} shows a slight red-shift, while in DEuPC, which has 22 carbons, the λ_{Max} is very red-shifted. The same trend is present when 30 mol% cholesterol is added, but to a slightly lesser extent.

As an alternate, complementary way of testing Trp1 depth in the bilayer, we examined quenching. We added one of two quenchers, 10-DN (10-doxylnonadecane) or acrylamide, to check if this was indeed the case. 10-DN only quenches fluorescence within the membrane, while acrylamide remains in the aqueous environment and

quenches fluorescent groups exposed to buffer. A useful rough measure of Trp depth is to measure the ratio of quenching by the two quenchers. A high value of acrylamide: 10-DN quenching suggests a Trp is closer to the surface, while a low value suggests that it is more deeply buried in the bilayer. In this experiment we added 10-DN to the peptide/lipid mix before forming the vesicles, ensuring that the 10-DN would be incorporated into the bilayers as the vesicles were formed, or added acrylamide to the aqueous buffer after the vesicles were formed. 10-DN does not absorb at 280 nm, so we were able to use the standard excitation wavelength of 280 nm, and therefore used an emission wavelength of 340 nm. However, acrylamide absorbs at 280 nm, so we used an excitation wavelength of 295, and therefore needed to use a slightly longer emission wavelength of 340 nm.

In order to obtain the values in Table 2.4, we measured the average fluorescence intensity over a period of 10 seconds at 340 nm (for the acrylamide treatment) or at 330 nm (for the 10-DN treatment) for each sample. Each treatment was compared to no treatment (that is, no quencher) and background (that is, no peptide) controls. To determine the degree of 10-DN quenching, the background control was first subtracted from both the average of the triplicate samples that included quencher and average of the triplicate samples without quencher to obtain the corrected fluorescence intensities (F). The F of the no treatment controls were then averaged to obtain the average fluorescence intensity (F_o). F_o was divided by the F of each 10-DN treatment sample and the results were averaged to obtain the average 10-DN F_o/F.

To determine the degree of acrylamide quenching, the background control was subtracted from triplicate samples to obtain F_1. Since acrylamide was added after vesicle

formation, we corrected for the extra volume of 50 µL ((850 µL/800 µL)*F_1) (the total volume was 850 µL, as opposed to 800µL in the samples without quencher), the acrylamide concentration (4.0 M*(50 µL/850 µL)), and for the absorbance due to acrylamide (0.1 = the correction factor for the inner filter) at 340 nm ($10^{(0.1 \text{ times } (4.0 \text{ M}*(50 \text{ µL}/850 \text{ µL})))}$) to obtain F_2. F_2 was then divided by F_1 to obtain F. The F values of the no treatment controls were averaged to obtain F_o. F_o was then divided by the F of each acrylamide treatment sampled and the results were averaged to obtain the average acrylamide F_o/F.

A value of 1 was subtracted from the average 10-DN and acrylamide F_o/F's to obtain the degrees of quenching, which are displayed as the degree of 10-DN quenching and the degree of acrylamid quenching in Table 2.4. The acrylamide degree of quenching was divided by the 10-DN degree of quenching to obtain the acrylamide:10-DN quenching ratio. As shown in Table 2.4, the acrylamide quenched 5-fold more of the fluorescence than 10-DN in DMoPC, while the 10-DN quenched 4-fold more of the fluorescence than acrylamide in DEuPC. These data indicated that the peptide may have existed in two different conformations, depending on the thickness of the bilayer into which it had inserted. The low quenching ratio in DEuPC bilayers is consistent with a low degree of buffer exposure, and a relatively deep Trp orientation. By contrast, the higher quenching ratio in DMoPC bilayers is consistent with a higher degree of buffer exposure and a much shallower Trp position in the bilayer. As detailed in the discussion, this result was surprising, especially for DEuPC bilayers, because it appeared to conflict with the λ_{max} data.

Lipid composition	Lipid + Peptide Fluorescence Intensity at 340 nm	Lipid + Peptide + Acrylamide Fluorescence Intensity at 340 nm	Lipid + Peptide Fluorescence Intensity at 330 nm	Lipid + Peptide + 10-DN Fluorescence Intensity at 330 nm	Quenching Ratio of acrylamide: 10-DN
DMoPC	$1.72\ 10^{06}$	$3.46\ 10^{05}$	$3.69\ 10^{06}$	$1.83\ 10^{06}$	4.919
Degree of Quenching $\frac{F_{(-quencher)}}{F_{(+quencher)}}$	n/a	5.08	n/a	1.03	n/a
DEuPC	$3.80\ 10^{05}$	$1.40\ 10^{05}$	$1.27\ 10^{06}$	$2.86\ 10^{05}$	0.259
Degree of Quenching $\frac{F_{(-quencher)}}{F_{(+quencher)}}$	n/a	0.92	n/a	3.55	n/a

Table 2.4. The effect of two quenchers, 10-DN and acrylamide, on the fluorescence of the caveolin-1 tryptophan. The fluorescence intensity for the lipid alone was 1.84 e^{05} for DMoPC and 7.27 e^{04} for DEuPC. The lipid + acrylamide fluorescence intensity was 1.17 e^{05} for DMoPC and 7.23 e^{05} for DEuPC. More fluorescence was quenched by acrylamide in DMoPC while 10-DN quenched more fluorescence in DEuPC.

Discussion:

We saw a difference in Trp1 λ_{max} in vesicles of different bilayer thicknesses, which indicated that the peptide acted differently in thin vs. thick bilayers. This result suggested that the dramatic flattening of caveolae seen in cells upon cholesterol depletion might simply result from the resulting reduction in membrane thickness, which might in turn change the way the caveolin-1 hydrophobic domain associated with the bilayer. However, the λ_{max} and quenching experiments appeared to contradict each other. The quenching data indicated that Trp1 was buried within the bilayer in thicker bilayers while the λ_{max} data for DEuPC indicated that Trp1 was in an aqueous environment. These contrasting results may be due to peptide aggregation where charged amino acid residues from other peptide moieties may be affecting the environment around Trp1. Unfortunately, there is no obvious explanation for these differing results at this time. Together, these data suggest that the caveolin-1 peptide behaves in an unusual manner that we do not yet fully understand.

Despite these uncertainties, it was clear that the caveolin-1 peptide appeared to adopt two different conformations depending on the thickness of the bilayer. A tentative working model for how this occurs, and for how caveolin-1 induces membrane curvature in thick bilayers but not thin ones, is as follows. Thinner membranes might allow the hydrophobic domain to form a hairpin loop, whereas the hydrophobic domain would be too short to form a hairpin in thicker membranes. A hairpin loop conformation would be unlikely to form in thicker membranes due to unsatisfied hydrogen bonds at the position of the turn, which are very energetically unfavorable in lipid bilayers. In DMoPC, which forms a bilayer with a hydrophobic core that is ~21Å thick (Lewis and Engleman, 1983),

only 15 amino acid residues are required to span the membrane. Since the hydrophobic region of caveolin-1 is 33 amino acid residues long, it can form a loop structure, which would place the Trp (located near the center of the hydrophobic region) in the border region of the membrane, allowing it to be quenched more by the acrylamide (Fig. 2.3A). This localization at the more hydrophilic membrane interface would help to stabilize the unsatisfied hydrogen bonds. In DEuPC, which forms a bilayer with a hydrophobic core that is ~35Å thick (Lewis and Engleman, 1983), the hydrophobic region cannot span the membrane while keeping both termini on the same side. Therefore, the peptide may adopt a conformation whereby the hydrophobic region is partially embedded into one layer of the bilayer with the tryptophan pointing down into the membrane (Fig. 2.3B). This conformation would result in the increased quenching by the 10-DN quencher that was observed.

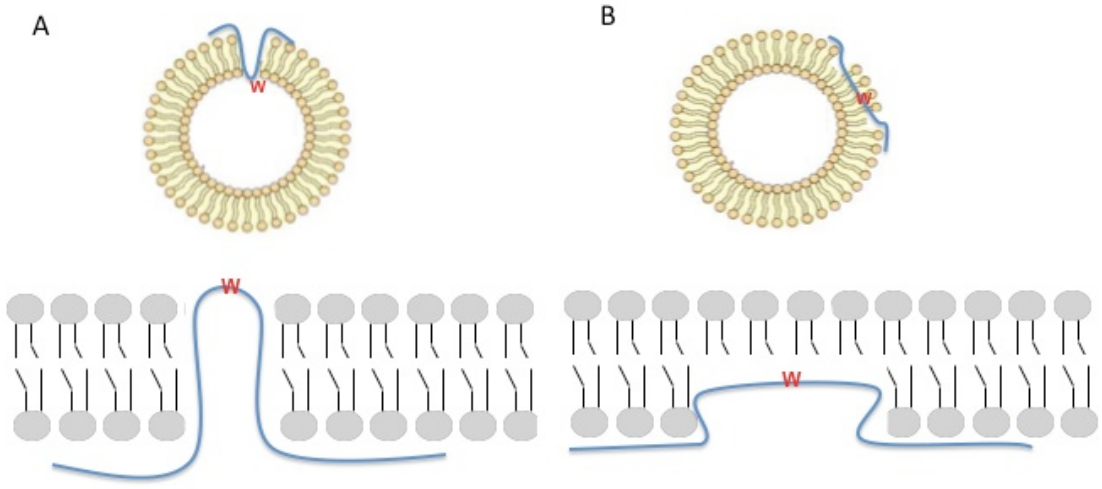

Figure 2.3. Putative caveolin-1 peptide conformation depending on bilayer thickness. The upper half of each panel shows a vesicle cross-section, and close-ups of each bilayer are shown in the bottom halves. A thin bilayer is shown in A, a thick bilayer is shown in B. The caveolin-1 peptide is in blue and red Trps indicate the probable location of Trp1 used to measure fluorescence.

This model fits the data fairly well for the peptide in DMoPC bilayers, although the quenching ratio is a bit higher than might be expected for a Trp at the membrane interface. However, the behavior of the peptide in DEuPC bilayers is hard to explain, and is not fully explained by this model. The λ_{max} results suggest that the Trp is highly solvent-exposed, while the quenching data suggests the opposite. It is likely that we do not yet fully understand the way the peptide is situated in these bilayers.

Although the addition of cholesterol did not appear to affect Trp1 λ_{max} in these vesicles, this may be due to the use of a simple modeling system. *In vivo*, another protein, cavin, is also required to form caveolae: caveolin-1 will not form caveolae in the absence of cavin (Hill et al., 2008; Liu et al., 2008; Liu and Pilch, 2008). Therefore, it is possible that caveolin-1 and cholesterol do not directly interact, and that cavin may in some way mediate the response of caveolin-1 to the presence or absence of cholesterol. In addition, it is unknown to what degree the addition of cholesterol alters the thickness of the membrane bilayer. Since the plasma membrane is formed mostly by 16- and 18-carbon chain phospholipids and glycolipids, although it also contains some 20-carbon chain lipids (Alberts et al., 2007), it is possible that cholesterol does not affect the bilayer thickness enough for the peptide to react in a noticeable manner.

We were pleased to find that the extra charges on either end of the caveolin-1 peptide appeared to prevent it from forming the transmembrane conformation with the termini on opposite sides of the bilayer, since *in vivo* the full-length protein has only one hydrophobic domain and both termini are on the same side of the bilayer (Uittenbogaard and Smart, 2000). We do not know why the peptide did not appear to become transmembraneous when added with lipids before vesicle formation. It's possible that the

particular sequence of the peptide favors formation of a central turn, disfavoring the transmembrane state. Alternatively, the peptide may self-associate to some degree even when added to lipids, slowing release of free peptide that's available to insert into membranes until after lipids have formed vesicles. Further work will be required to fully understand the behavior of this intriguing peptide.

References:

Alberts, B., A. Johnson, J. Lews, M. Raff, K. Roberts, and P. Walter. 2007. Molecular Biology of the Cell. Garland Science, New York, NY.

Bonifacino, J.S., and J. Lippincott-Schwartz. 2003. Coat proteins: shaping membrane transport. *Nat Rev Mol Cell Biol*. 4:409-414.

Caputo, G.A., and E. London. 2004. Position and ionization state of Asp in the core of membrane-inserted alpha helices control both the equilibrium between transmembrane and nontransmembrane helix topography and transmembrane helix positioning. *Biochemistry*. 43:8794-8806.

Farsad, K., and P.D. Camilli. 2003. Mechanisms of membrane deformation. *Current Opinion in Cell Biology*. 15:372-381.

Ford, M.G.J., I.G. Mills, B.J. Peter, Y. Vallis, G.J.K. Praefcke, P.R. Evans, and H.T. McMahon. 2002. Curvature of clathrin-coated pits driven by epsin. *Nature*. 419:361-366.

Gallop, J., and H. McMahon. 2005. BAR domains and membrane curvature: bringing your curves to the BAR. *Biochem Soc Symp*. 72:223-231.

Hill, M.M., M. Bastiani, R. Luetterforst, M. Kirkham, A. Kirkham, S.J. Nixon, P. Walser, D. Abankwa, V.M.J. Oorschot, S. Martin, J.F. Hancock, and R.G. Parton. 2008. PTRF-cavin, a conserved cytoplasmic protein required for caveola formation and function. *Cell*. 132:113-124.

Hu, J., Y. Shibata, C. Voss, T. Shemesh, Z. Li, M. Coughlin, M.M. Kozlov, T.A. Rapoport, and W.A. Prinz. 2008. Membrane proteins of the endoplasmic reticulum induce high-curvature tubules. *Science*. 319:1247-1250.

Lewis, B.A., and D.M. Engleman. 1983. Bacteriorhodopsin remains dispersed in fluid phospholipid bilayers over a wide range of bilayer thicknesses. *Journal of Molecular Biology*. 166:203-210.

Liu, L., D. Brown, M. McKee, N.K. LeBrasseur, D. Yang, K.H. Albrecht, K. Ravid, and P.F. Pilch. 2008. Deletion of cavin/PTRF causes global goss of caveolae, dyslipidemia, and glucose intolerance. *Cell Metabolism*. 8:310-317.

Liu, L., and P.F. Pilch. 2008. A critical role of cavin (polymerase I and transcript release factor) in caveolae formation and organization. *J. Biol. Chem.* 283:4314-4322.

Peter, B.J., H.M. Kent, I.G. Mills, Y. Vallis, P.J.G. Butler, P.R. Evans, and H.T. McMahon. 2004. BAR domains as sensors of membrane curvature: the amphiphysin BAR structure. *Science*. 303:495-499.

Polishchuk, R.S., E.V. Polishchuk, P. Marra, S. Alberti, R. Buccione, A. Luini, and A.A. Mironov. 2000. Correlative light-electron microscopy reveals the tubular-saccular ultrastructure of carriers operating between Golgi apparatus and plasma membrane. *J. Cell Biol.* 148:45-58.

Shahidullah, K., and E. London. 2008. Effect of lipid composition on the topography of membrane-associated hydrophobic helices: stabilization of transmembrane topography by anionic lipids. *Journal of Molecular Biology*. 379:704-718.

Tagawa, A., A. Mezzacasa, A. Hayer, A. Longatti, L. Pelkmans, and A. Helenius. 2005. Assembly and trafficking of caveolar domains in the cell: caveolae as stable, cargo-triggered, vesicular transporters. *J. Cell Biol.* 170:769-779.

Uittenbogaard, A., and E.J. Smart. 2000. Palmitoylation of caveolin-1 is required for cholesterol binding, chaperone complex formation, and rapid transport of cholesterol to caveolae. *J. Biol. Chem.* 275:25595-25599.

Voeltz, G.K., W.A. Prinz, Y. Shibata, J.M. Rist, and T.A. Rapoport. 2006. A class of membrane proteins shaping the tubular endoplasmic reticulum. *Cell*. 124:573 - 586.

Zimmerberg, J., and M.M. Kozlov. 2006. How proteins produce cellular membrane curvature. *Nat Rev Mol Cell Biol*. 7:9-19.

Comprehensive List of References:

Alberts, B., A. Johnson, J. Lews, M. Raff, K. Roberts, and P. Walter. 2007. Molecular Biology of the Cell. Garland Science, New York, NY.

Bonifacino, J.S., and J. Lippincott-Schwartz. 2003. Coat proteins: shaping membrane transport. *Nat Rev Mol Cell Biol*. 4:409-414.

Brodsky, F.M., C.-Y. Chen, C. Knuehl, M.C. Towler, and D.E. Wakeham. 2001. Biological basket weaving: formation and function of clathrin-coated vesicles. *Annual Review of Cell and Developmental Biology*. 17:517-568.

Caputo, G.A., and E. London. 2004. Position and ionization state of Asp in the core of membrane-inserted alpha helices control both the equilibrium between transmembrane and nontransmembrane helix topography and transmembrane helix positioning. *Biochemistry*. 43:8794-8806.

Conner, S.D., and S.L. Schmid. 2003. Regulated portals of entry into the cell. *Nature*. 422:37-44.

Doherty, G.J., and H.T. McMahon. 2009. Mechanisms of endocytosis. *Annual Review of Biochemistry*. 78.

Farsad, K., and P.D. Camilli. 2003. Mechanisms of membrane deformation. *Current Opinion in Cell Biology*. 15:372-381.

Ford, M.G.J., I.G. Mills, B.J. Peter, Y. Vallis, G.J.K. Praefcke, P.R. Evans, and H.T. McMahon. 2002. Curvature of clathrin-coated pits driven by epsin. *Nature*. 419:361-366.

Gallop, J., and H. McMahon. 2005. BAR domains and membrane curvature: bringing your curves to the BAR. *Biochem Soc Symp*. 72:223-231.

Ghosh, R.N., W.G. Mallet, T.T. Soe, T.E. McGraw, and F.R. Maxfield. 1998. An endocytosed TGN38 chimeric protein is delivered to the TGN after trafficking through the endocytic recycling compartment in CHO Cells. *J. Cell Biol.* 142:923-936.

Guillot, F.L., K.L. Audus, and T.J. Raub. 1990. Fluid-phase endocytosis by primary cultures of bovine brain microvessel endothelial cell monolayers. *Microvascular Research*. 39:1-14.

Hazes, B., and R.J. Read. 1997. Accumulating evidence suggests that several AB-toxins subvert the endoplasmic reticulum-associated protein degradation pathway to enter target cells. *Biochemistry*. 36:11051-11054.

Hill, M.M., M. Bastiani, R. Luetterforst, M. Kirkham, A. Kirkham, S.J. Nixon, P. Walser, D. Abankwa, V.M.J. Oorschot, S. Martin, J.F. Hancock, and R.G. Parton. 2008. PTRF-cavin, a conserved cytoplasmic protein required for caveola formation and function. *Cell*. 132:113-124.

Hu, J., Y. Shibata, C. Voss, T. Shemesh, Z. Li, M. Coughlin, M.M. Kozlov, T.A. Rapoport, and W.A. Prinz. 2008. Membrane proteins of the endoplasmic reticulum induce high-curvature tubules. *Science*. 319:1247-1250.

Johannes, L., and V. Popoff. 2008. Tracing the retrograde route in protein trafficking. *Cell*. 135:1175-1187.

Johnson, A., R. Ghosh, K. Dunn, R. Garippa, J. Park, S. Mayor, F. Maxfield, and T. McGraw. 1996. Transferrin receptor containing the SDYQRL motif of TGN38

causes a reorganization of the recycling compartment but is not targeted to the TGN. *J. Cell Biol.* 135:1749-1762.

Lencer, W.I., and B. Tsai. 2003. The intracellular voyage of cholera toxin: going retro. *Trends in Biochemical Sciences*. 28:639-645.

Lewis, B.A., and D.M. Engleman. 1983. Bacteriorhodopsin remains dispersed in fluid phospholipid bilayers over a wide range of bilayer thicknesses. *Journal of Molecular Biology*. 166:203-210.

Liu, L., D. Brown, M. McKee, N.K. LeBrasseur, D. Yang, K.H. Albrecht, K. Ravid, and P.F. Pilch. 2008. Deletion of cavin/PTRF causes global goss of caveolae, dyslipidemia, and glucose intolerance. *Cell Metabolism*. 8:310-317.

Liu, L., and P.F. Pilch. 2008. A critical role of cavin (polymerase I and transcript release factor) in caveolae formation and organization. *J. Biol. Chem.* 283:4314-4322.

Majoul, I., K. Sohn, F.T. Wieland, R. Pepperkok, M. Pizza, J. Hillemann, and H.-D. Soling. 1998. KDEL receptor (Erd2p)-mediated retrograde transport of the cholera toxin A subunit from the Golgi involves COPI, p23, and the COOH terminus of Erd2p. *J. Cell Biol.* 143:601-612.

Majoul, I.V., P.I.H. Bastiaens, and H.-D. Soling. 1996. Transport of an external Lys-Asp-Glu-Leu (KDEL) protein from the plasma membrane to the endoplasmic reticulum: studies with cholera toxin in Vero cells. *J. Cell Biol.* 133:777.

Mundy, D.I., T. Machleidt, Y.-s. Ying, R.G.W. Anderson, and G.S. Bloom. 2002. Dual control of caveolar membrane traffic by microtubules and the actin cytoskeleton. *J Cell Sci*. 115:4327-4339.

Nichols, B. 2003. Caveosomes and endocytosis of lipid rafts. *J Cell Sci*. 116:4707-4714.

Parton, R.G., and A.A. Richards. 2003. Lipid rafts and caveolae as portals for endocytosis: new insights and common mechanisms. *Traffic*. 4:724-738.

Parton, R.G., and K. Simons. 2007. The multiple faces of caveolae. *Nat Rev Mol Cell Biol*. 8:185-194.

Pelkmans, L., T. B¸rli, M. Zerial, and A. Helenius. 2004. Caveolin-stabilized membrane domains as multifunctional transport and sorting devices in endocytic membrane traffic. *Cell*. 118:767-780.

Pelkmans, L., and M. Zerial. 2005. Kinase-regulated quantal assemblies and kiss-and-run recycling of caveolae. *Nature*. 436:128-133.

Peter, B.J., H.M. Kent, I.G. Mills, Y. Vallis, P.J.G. Butler, P.R. Evans, and H.T. McMahon. 2004. BAR domains as sensors of membrane curvature: the amphiphysin BAR structure. *Science*. 303:495-499.

Polishchuk, R.S., E.V. Polishchuk, P. Marra, S. Alberti, R. Buccione, A. Luini, and A.A. Mironov. 2000. Correlative light-electron microscopy reveals the tubular-saccular ultrastructure of carriers operating between Golgi apparatus and plasma membrane. *J. Cell Biol.* 148:45-58.

Popoff, V., G.A. Mardones, D. Tenza, R. Rojas, C. Lamaze, J.S. Bonifacino, G. Raposo, and L. Johannes. 2007. The retromer complex and clathrin define an early endosomal retrograde exit site. *J Cell Sci*. 120:2022-2031.

Ren, X., A.G. Ostermeyer, L.T. Ramcharan, Y. Zeng, D.M. Lublin, and D.A. Brown. 2004. Conformational defects slow Golgi exit, block oligomerization, and reduce raft affinity of caveolin-1 mutant proteins. *Mol. Biol. Cell*. 15:4556-4567.

Richards, A.A., E. Stang, R. Pepperkok, and R.G. Parton. 2002. Inhibitors of COP-mediated transport and cholera toxin action inhibit simian virus 40 infection. *Mol. Biol. Cell*. 13:1750-1764.

Ridley, A.J. 2001. Rho proteins: linking signaling with membrane trafficking. *Traffic*. 2:303-310.

Rothberg, K.G., J.E. Heuser, W.C. Donzell, Y.-S. Ying, J.R. Glenney, and R.G.W. Anderson. 1992. Caveolin, a protein component of caveolae membrane coats. *Cell*. 68:673-682.

Sandvig, K., and B. van Deurs. 2002. Membrane traffic exploited by protein toxins. *Annual Review of Cell and Developmental Biology*. 18:1-24.

Shahidullah, K., and E. London. 2008. Effect of lipid composition on the topography of membrane-associated hydrophobic helices: stabilization of transmembrane topography by anionic lipids. *Journal of Molecular Biology*. 379:704-718.

Sorkin, A., and L.K. Goh. 2008. Endocytosis and intracellular trafficking of ErbBs. *Exp Cell Res*. 314:3093-3106.

Tagawa, A., A. Mezzacasa, A. Hayer, A. Longatti, L. Pelkmans, and A. Helenius. 2005. Assembly and trafficking of caveolar domains in the cell: caveolae as stable, cargo-triggered, vesicular transporters. *J. Cell Biol.* 170:769-779.

Thomas, C.M., and E.J. Smart. 2008. Caveolae structure and function. *Journal of Cellular and Molecular Medicine*. 12:796-809.

Thorn, H., K.G. Stenkula, M. Karlsson, U. Ortegren, F.H. Nystrom, J. Gustavsson, and P. Stralfors. 2003. Cell surface orifices of caveolae and localization of caveolin to the necks of caveolae in adipocytes. *Mol. Biol. Cell*. 14:3967-3976.

Tsai, B., Y. Ye, and T.A. Rapoport. 2002. Retro-translocation of proteins from the endoplasmic reticulum into the cytosol. *Nat Rev Mol Cell Biol*. 3:246-255.

Uittenbogaard, A., and E.J. Smart. 2000. Palmitoylation of caveolin-1 is required for cholesterol binding, chaperone complex formation, and rapid transport of cholesterol to caveolae. *J. Biol. Chem.* 275:25595-25599.

Voeltz, G.K., W.A. Prinz, Y. Shibata, J.M. Rist, and T.A. Rapoport. 2006. A class of membrane proteins shaping the tubular endoplasmic reticulum. *Cell*. 124:573 - 586.

Xie, Z., X. Zeng, T. Waldman, and R.I. Glazer. 2003. Transformation of mammary epithelial cells by 3-phosphoinositide-dependent protein kinase-1 activates {beta}-catenin and c-Myc, and down-regulates caveolin-1. *Cancer Res*. 63:5370-5375.

Zimmerberg, J., and M.M. Kozlov. 2006. How proteins produce cellular membrane curvature. *Nat Rev Mol Cell Biol*. 7:9-1